METEOROLOGICAL OFFICE

HADLEY CENTRE
FOR CLIMATE PREDICTION AND RESEARCH

Middle Atmosphere Variability in the UKMO Unified Model

by

R Swinbank, W Lahoz, C Douglas
A Heaps, R Brugge, W Norton, A O'Neill, D Podd

CRTN 76

November 1996

CLIMATE
RESEARCH
TECHNICAL
NOTE

Hadley Centre
Meteorological Office
London Road
Bracknell
Berkshire RG12 2SY

CLIMATE RESEARCH TECHNICAL NOTE NO. 76

MIDDLE ATMOSPHERE VARIABILITY IN THE UKMO UNIFIED MODEL

by

R Swinbank, W Lahoz,
C Douglas, A Heaps, R Brugge, W Norton, A O'Neill, D Podd

This paper is also being issued as
UGAMP Technical Report No. 42

Hadley Centre for Climate Prediction and Research
Meteorological Office
London Road
Bracknell
Berkshire RG12 2SY

NOTE: This paper has not been published. Permission to quote from it should be obtained from the Director of the Hadley Centre.

CLIMATE RESEARCH TECHNICAL NOTE NO. 76

MIDDLE ATMOSPHERE VARIABILITY IN THE UKMO UNIFIED MODEL

by

R Swinbank, W Lahoz,
C Douglas, A Heaps, R Brugge, W Norton, A O'Neill, D Podd

This paper is also being issued as
UGAMP Technical Report No. 42

Hadley Centre for Climate Prediction and Research
Meteorological Office
London Road
Bracknell
Berkshire RG12 2SY

NOTE: This paper has not been published. Permission to quote from it should be obtained from the Director of the Hadley Centre.

1. Introduction

This technical note describes a stratosphere-troposphere version of the UK Meteorological Office (UKMO) Unified Model (UM) (Cullen 1993). General circulation modelling has historically concentrated on the simulation of the atmospheric circulation in the troposphere. During the last decade two approaches have been used in middle atmosphere modelling studies. The first approach uses General Circulation Models (GCMs) which have been extended to encompass the stratosphere as well as the troposphere, notably the Geophysical Fluid Dynamics Laboratory (GFDL) SKYHI model (Hamilton et al. 1995) and the National Center for Atmospheric Research (NCAR) Community Climate Model (Boville 1995). The second approach uses models with a prescribed lower boundary condition near the tropopause (e.g. the UKMO Stratosphere-Mesosphere Model, Fisher 1987). Using a GCM which spans the troposphere and the stratosphere has the advantage that the model simulations are consistent throughout the lower and middle atmosphere. A stratosphere-troposphere configuration of the UM with 42 levels was originally developed in conjunction with the Upper Atmosphere Research Satellite (UARS) stratospheric data assimilation system (Swinbank and O'Neill 1994). The 49 level model described in this technical note extends to a higher level in the lower mesosphere, and its main use is in longer simulations of the stratospheric circulation.

Although the stratosphere may have little impact on short-term tropospheric forecasts, improvements to the representation of the stratosphere in the model are likely to have an impact on the skill of medium range and longer term simulations. Operational numerical weather prediction models extend to higher levels than they did a decade ago, and we anticipate that the trend whereby models are extended upwards will continue. The experimental use of GCMs extending throughout the stratosphere will contribute to the future development of Numerical Weather Prediction and Climate models with extended vertical coverage.

2. Model description

2.1 General information

The Unified Model is the name given to a suite of numerical modelling software developed and used at the UKMO. The model is designed to be used for a wide range of different applications -- notably Numerical Weather Prediction and climate simulation. The modelling system also includes an ocean model, which can be run coupled with the atmosphere model, and a data assimilation scheme to assimilate meteorological observations. The Unified Model was introduced into operational service in 1991. Since then both its formulation and capabilities have been substantially enhanced.

The choice of horizontal and vertical resolution is arbitrary, although a number of standard resolutions tend to be used. Both the operational and climate models are currently run using a

set of 19 levels, extending up to the middle stratosphere; the vertical resolution used for the top few levels is quite coarse (typically 5 km). By contrast, the 49-level configuration is designed to have a high vertical resolution of approximately 1.3 km throughout the stratosphere. The Unified Model uses a hybrid pressure/sigma vertical coordinate system (Simmons and Strüfing 1983). The lowest four model levels are sigma levels, and the model levels gradually become constant pressure surfaces above about 50 hPa (see Table 1 and Figure 1).

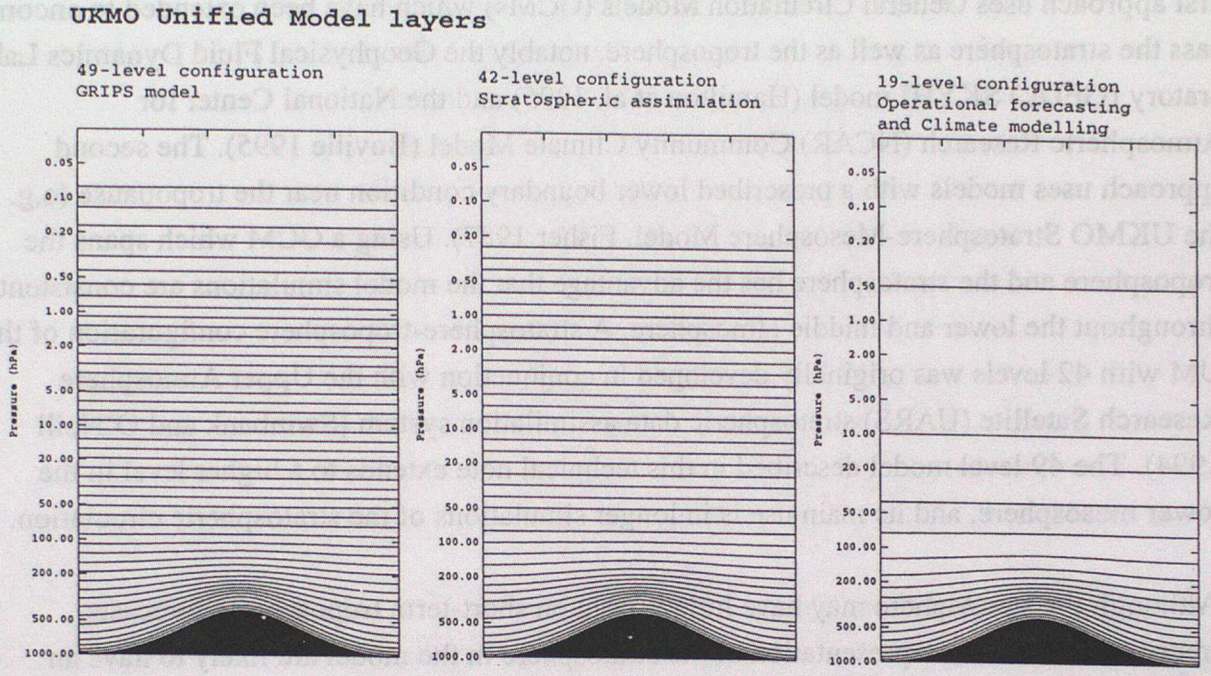

Fig 1. Model levels for three different UM configurations
(GRIPS is the GCM Reality Intercomparison Project for SPARC).

The Unified Model is grid-point and has a global domain with a horizontal resolution of 2.5° latitude and 3.75° longitude. This is the same resolution as that usually used for climate modelling, but three times coarser than the current operational resolution used for global forecasting.

2.2 Dynamical processes

The model equations are based on the hydrostatic primitive equations. An efficient split-explicit scheme is used to solve the equations, which is designed to conserve mass, mass-weighted potential temperature, moisture and angular momentum. As a consequence of the formulation of the dynamics, the model variables are carried on a staggered (Arakawa B) grid. For further details of the representation of dynamical processes, see Table 2.

2.3 Physical Processes

A description of the physical parametrization schemes is given in Table 3. In brief, the set of

schemes used for the simulation described in this technical note are based on those used in the 'Third Climate Version' of the climate model used by the Hadley Centre (also known as HADAM2b). In order to run the model satisfactorily in the stratosphere, some changes were made to the radiation and orographic gravity wave drag schemes. The standard UM long-wave radiation scheme was modified so that the effects of major trace gases are treated in a similar way to that used by the European Centre for Medium Range Weather Forecasts (ECMWF) (see Morcrette et al., 1986 for details). The behaviour of the orographic gravity wave drag scheme was not sufficiently smooth in time and space and it was replaced above 20 hPa by a simple Rayleigh friction scheme, in which the winds are damped towards zero using a damping coefficient that depends on model level (see Figure 2). The Rayleigh drag acts almost exclusively in the mesosphere; the drag is rather more than would be given by gravity wave drag, in order to provide sufficient descent in the upper stratosphere over the winter pole. If the model lid were higher, so that the descent could build up over a deeper layer, it would be appropriate to use a profile more like the Middle Atmosphere version of the NCAR CCM2 model (see Figure 2).

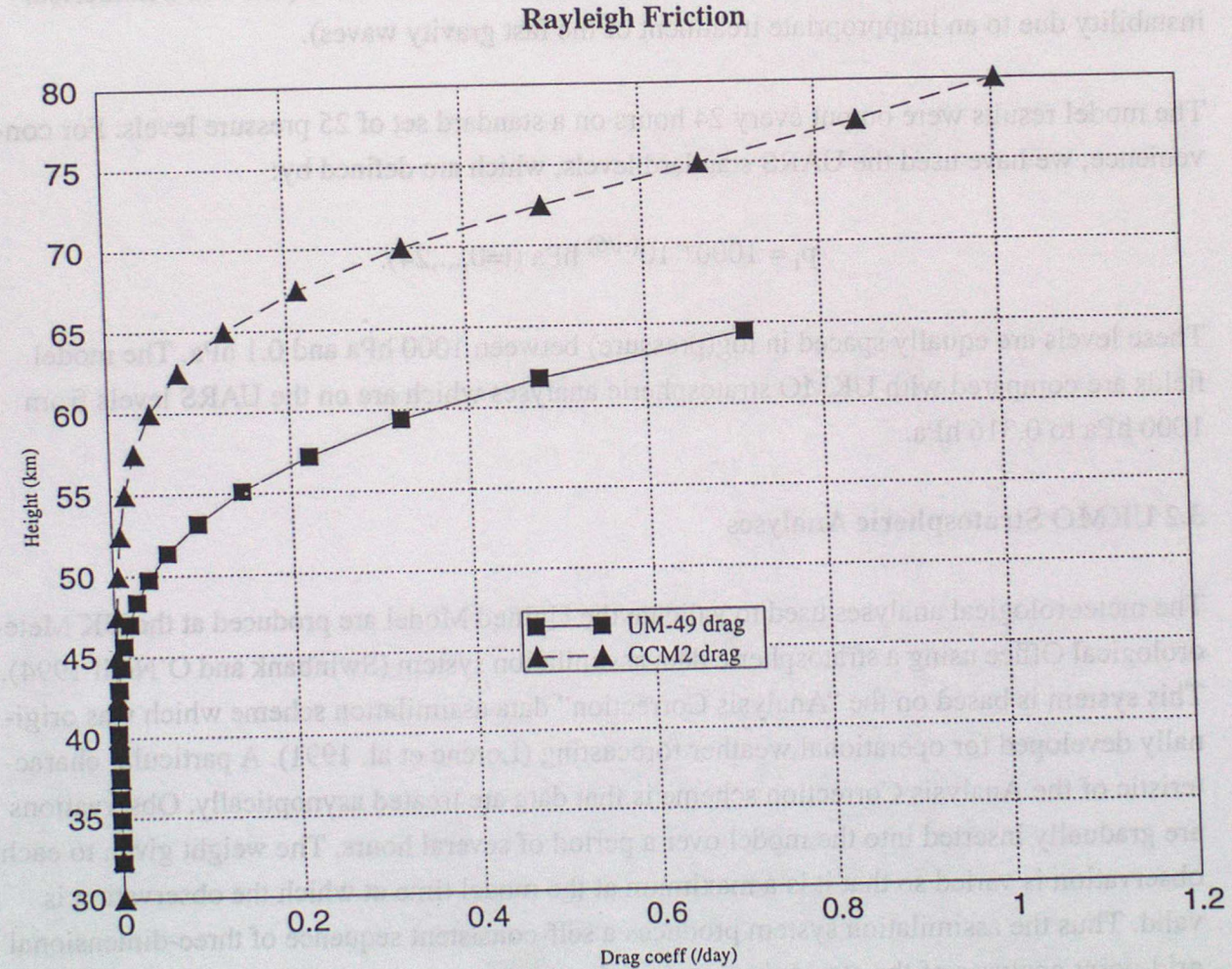

Fig 2. Rayleigh friction coefficient used in the 49-level version of the UM and the NCAR CCM2.

3. Data

3.1 Model Integrations

Several integrations have now been run in the course of developing the 49-level configuration of the Unified Model. We devote the remainder of the technical report to a presentation of the results from one of the latest simulations. The experiment has been carried out in a collaboration between the Centre for Global Atmospheric Modelling (CGAM) at the University of Reading and the UK Meteorological Office (UKMO). The experiment was started from the analysis valid at 12 GMT 10 April 1992 produced by the UKMO stratosphere-troposphere data assimilation system. Note that the model simulation described here uses the Gregorian calendar, starting from the initial date of 10 April 1992. The initial data was interpolated from the original 42 assimilation model levels to the 49 levels; the upper levels of the initial dataset (above 1 hPa) were produced by a combination of the analysed values and climatological values. The experiment finished on the model date of 2 August 1993, when the model integration failed. The cause of the failure has since been identified and corrected (this was a numerical instability due to an inappropriate treatment of the fast gravity waves).

The model results were output every 24 hours on a standard set of 25 pressure levels. For convenience, we have used the UARS standard levels, which are defined by:

$$p_i = 1000 * 10^{(-i/6)} \text{ hPa } (i=0,...,24).$$

These levels are equally spaced in log(pressure) between 1000 hPa and 0.1 hPa. The model fields are compared with UKMO stratospheric analyses which are on the UARS levels from 1000 hPa to 0.316 hPa.

3.2 UKMO Stratospheric Analyses

The meteorological analyses used to validate the Unified Model are produced at the UK Meteorological Office using a stratospheric data assimilation system (Swinbank and O'Neill 1994). This system is based on the "Analysis Correction" data assimilation scheme which was originally developed for operational weather forecasting (Lorenc et al. 1991). A particular characteristic of the Analysis Correction scheme is that data are treated asynoptically. Observations are gradually inserted into the model over a period of several hours. The weight given to each observation is varied so that it is a maximum at the model time at which the observation is valid. Thus the assimilation system produces a self-consistent sequence of three-dimensional grid-point analyses of the atmosphere, using observations to constrain the evolution of the Unified Model.

The UKMO analyses consist of daily global fields of temperature, geopotential height and

three-component winds. The assimilation uses a 42-level configuration of the Unified Model. Like the 49-level configuration, the horizontal resolution is 2.5° latitude by 3.75° longitude, but the vertical resolution is about 1.6 km in the stratosphere, with a top level at around 0.3 hPa (see Figure 1). The analyses are interpolated to the same UARS pressure levels as the model results. However, even though the top analysis level is 0.32 hPa, it should be borne in mind that the analyses are only reliable up to about 1 hPa; above this level they are significantly affected by errors associated with the model lid.

In this technical report we assess the model by comparing diagnostics from the model runs with equivalent diagnostics from the analyses. For example, the evolution of the simulated circulation through the winter is compared with the evolution for a particular winter from the UKMO analyses. This gives a better illustration of the model's ability to give a realistic simulation than, for example, a comparison with the mean of all available winters from the analyses. Since the model run is relatively short, it is not possible to satisfactorily compare the model simulation with the observed climatology. Indeed, since the UKMO analysis dataset is only about 5 years long, the observed climatology itself is not well determined.

3.3 Other model data

In this technical note we also compare the UM with the Extended UGAMP GCM (EUGCM -- see Gray et al. 1993). The EUGCM integrates the hydrostatic equations primitive equations over the globe from the ground to about 95-100 km (the exact height of the model pressure level depends on the temperatures below). The model is spectral; the main prognostic variables, vorticity, divergence, temperature, moisture and logarithm of surface pressure are represented as truncated series of spherical harmonics. The model has 47 levels in the vertical. The finite difference representation in the vertical is based on a hybrid sigma-pressure coordinate; the vertical spacing is about 2 km in the lower stratosphere, increasing to about 3 km near the mesopause.

Two radiation schemes are used in the EUGCM: the Morcrette (1990) scheme in the troposphere and lower stratosphere and the MIDRAD scheme (Shine 1987, Shine and Rickaby 1989) at higher altitudes, with a crude blending of the heating rates from the two schemes at around 74 hPa. The effects of unresolved gravity waves are represented by a scheme with a number of monochromatic noninteracting waves in each column (see Norton and Thuburn 1996 for more details). Other parametrized processes include convection (Betts and Miller 1993), large scale condensation, boundary layer processes and surface processes.

4. Model results

4.1 Seasonal evolution

In this section we have chosen, for convenience, to compare the UM simulation with the equivalent months from the UKMO analyses. Figure 3 shows the monthly zonal mean cross-section (latitude versus pressure) of zonal wind and temperature for January 1993 for the UM (top panel) and the UKMO analyses (bottom panel). The structure of the polar night jet in the UM cross-section is similar to that in the analysis cross-section, although the UM jet

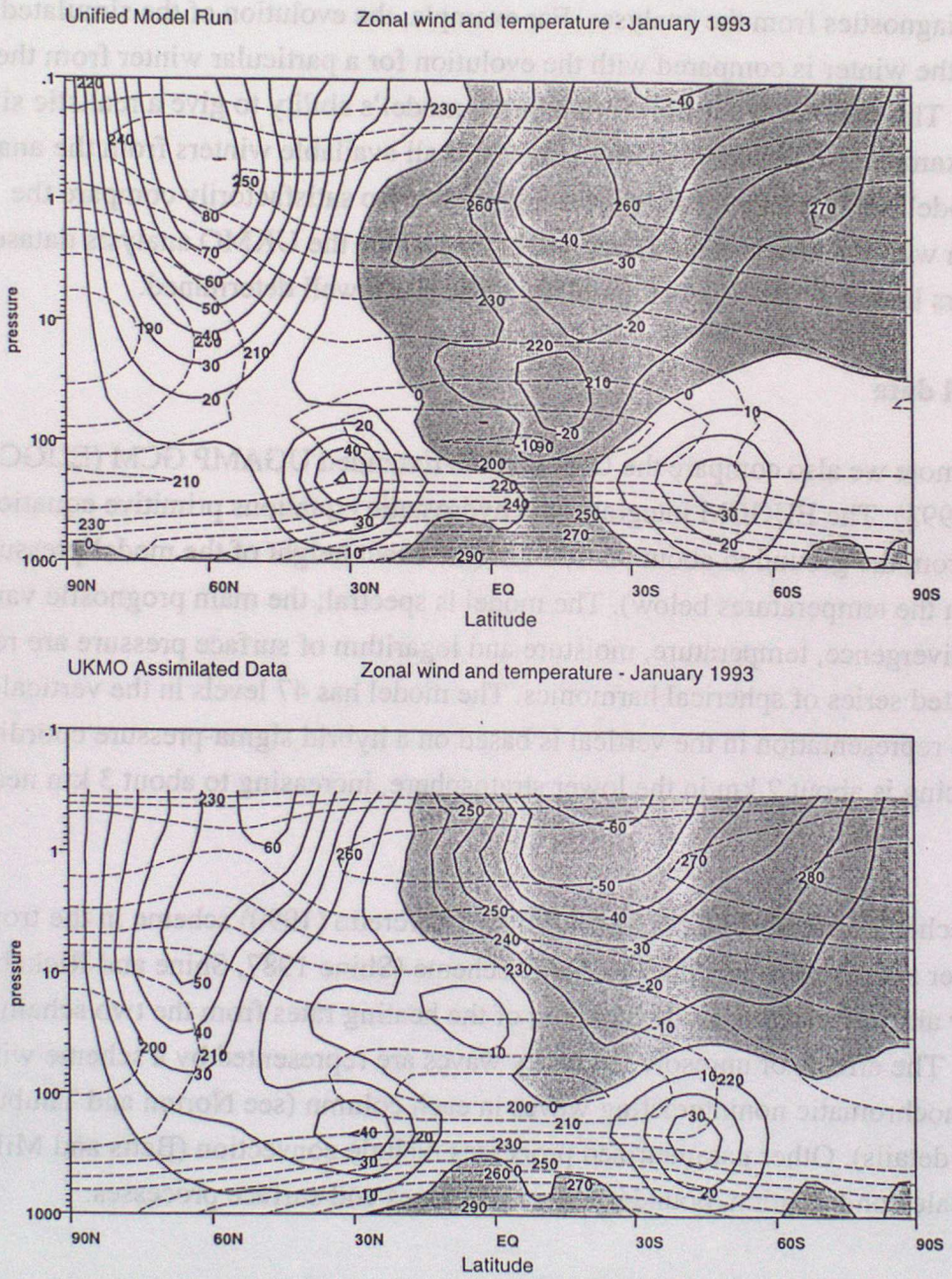

Fig 3. Monthly mean (latitude v pressure) of zonal wind (m/s -- solid contours) and temperature (K -- dashed contours) for January 1993 for the UM (top panel) and the UKMO analysis (bottom panel). The shading indicates easterly winds (negative values of the zonal wind).

(at about 80 m/s) was stronger than that in the UKMO analysis (about 60 m/s). The January zonal mean winds show considerable interannual variations; of the five Januarys in the UKMO analysis dataset, 1993 was the closest to the UM results. In January 1993 the simulation and analyses are similar, especially in the lower stratosphere; this suggests that the differences in the middle and upper stratosphere may be due to model biases at these levels rather than interannual variations.

The zonal mean differences in zonal wind and temperature are shown in Figure 4. Observations from the UKMO analysis indicate that the polar night jet tilts equatorward with height. On the other hand, this figure clearly shows the UM produced stronger winds at higher latitudes and upper levels, consistent with the model simulating an upright polar night jet. One possible reason for this is that the UM tends not to displace the polar vortex as far off the pole as one might expect when the stratosphere is disturbed, due to shortcomings in the way the polar singularity is treated by the model (all fields are filtered severely to remove waves shorter than the minimum wavelength which would be stable according to the CFL criterion). Another possible reason is the use of Rayleigh Friction to parametrize gravity wave drag. Experiments with the EUGCM (see section 3.3) suggest that this behaviour can be alleviated by using a more sophisticated gravity wave drag scheme (J. Thuburn pers. comm.).

Coupled with the stronger jet, the UM was colder than the UKMO analysis at high northern winter latitudes, by up to about 40 K near 3 hPa. This error has been found in other integrations with this configuration of the UM, so probably cannot be attributed to interannual variability.

The subtropical jets in the UM were closed and confined to mid latitudes. Their magnitudes were similar to those in the UKMO analysis; however, they were displaced poleward and extended higher into the lower stratosphere in the UM. In the southern (summer) hemisphere stratosphere, the structure of the winds in the UM was quite similar to the analyses, at least below 1 hPa. The simulated easterlies were about 10 m/s weaker than observed in the upper stratosphere. The differences are larger at upper levels; the UM winds tilted poleward whereas the analysed winds tilted equatorward. However these differences may not be significant, since the analyses are not reliable above about 1 hPa.

The Quasi-Biennial Oscillation (QBO) was in a westerly phase during January 1993; this was captured by the UKMO analysis, but the UM (in common with other middle atmosphere GCMs) was not able to simulate the QBO in the tropical stratosphere, so that in the lower and middle stratosphere of the UM, the simulated tropical winds were easterly rather than westerly. Instead, the model has retained the easterlies that were in the initial data used for the integration. Near the stratopause the analysed winds were easterly during January 1993, corresponding to the easterly phase of the Semi-Annual Oscillation (SAO). The UM had an SAO near the stratopause, but the oscillation did not reverse the winds (which were easterly).

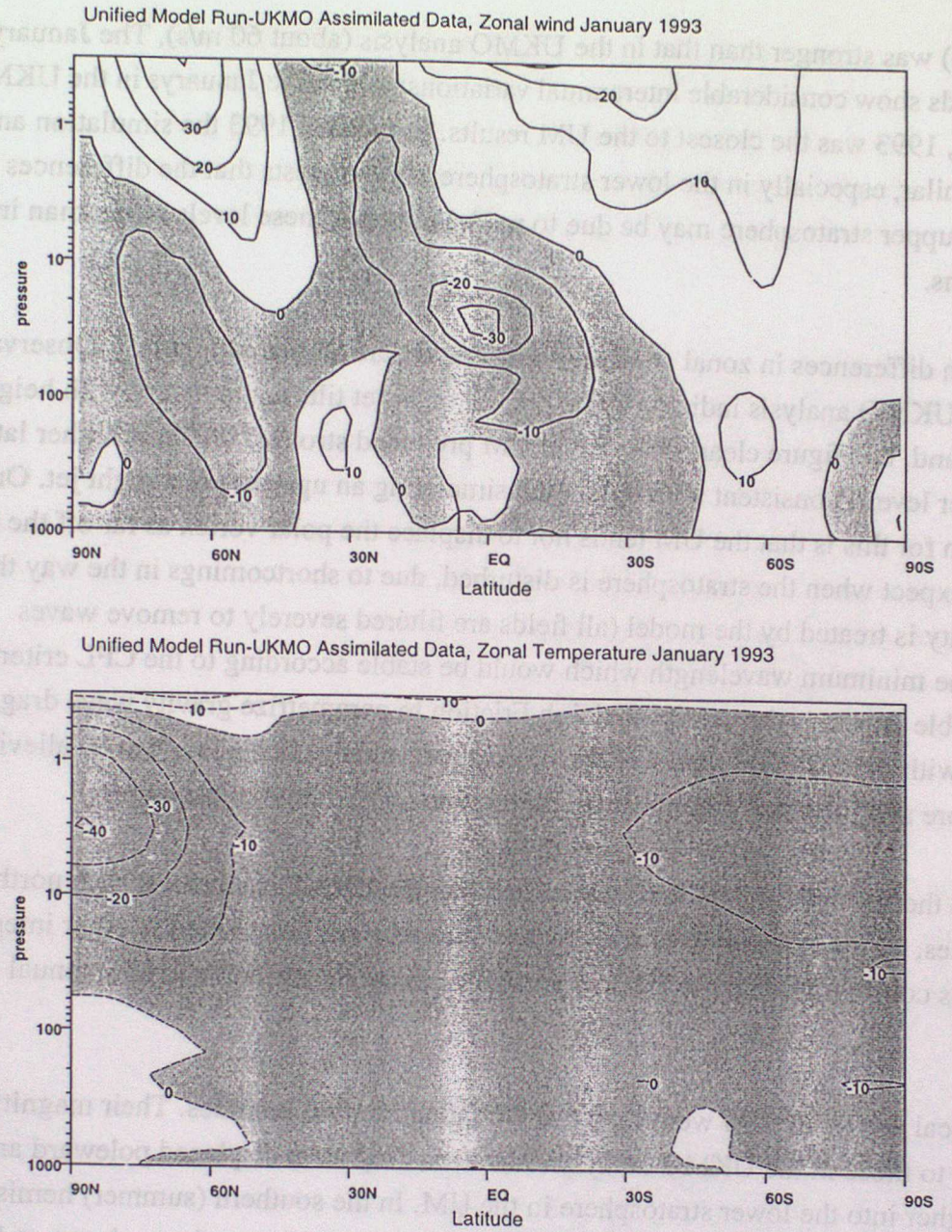

Fig. 4. Latitude-pressure cross-section of the difference between the UM model monthly mean and the UKMO analysis monthly mean for January 1993 zonal wind (m/s -- top panel) and temperature (K -- bottom panel). The difference field has shading in the regions where the UM values are lower than the UKMO analysis values.

Figure 5 shows the monthly zonal cross-sections of zonal wind and temperature for July 1992 for the UM simulation and the UKMO analysis, and Figure 6 shows cross-sections of the differences between the two datasets. As in January, the polar night jet in the UM (values about 100 m/s) was stronger than that in the analysis (values about 90 m/s). Once again, the biggest differences were at high latitudes at upper levels. The polar night jet was upright and did not tilt equatorward (but there was only a slight tilt in the July analyses, compared to the equivalent January jet). Consistent with the bias in the jet, the UM was significantly colder, by up to 30 K, than the UKMO analysis at high southern latitudes. In contrast to January, the July zonal mean fields show little interannual variability, so the differences found here can be more

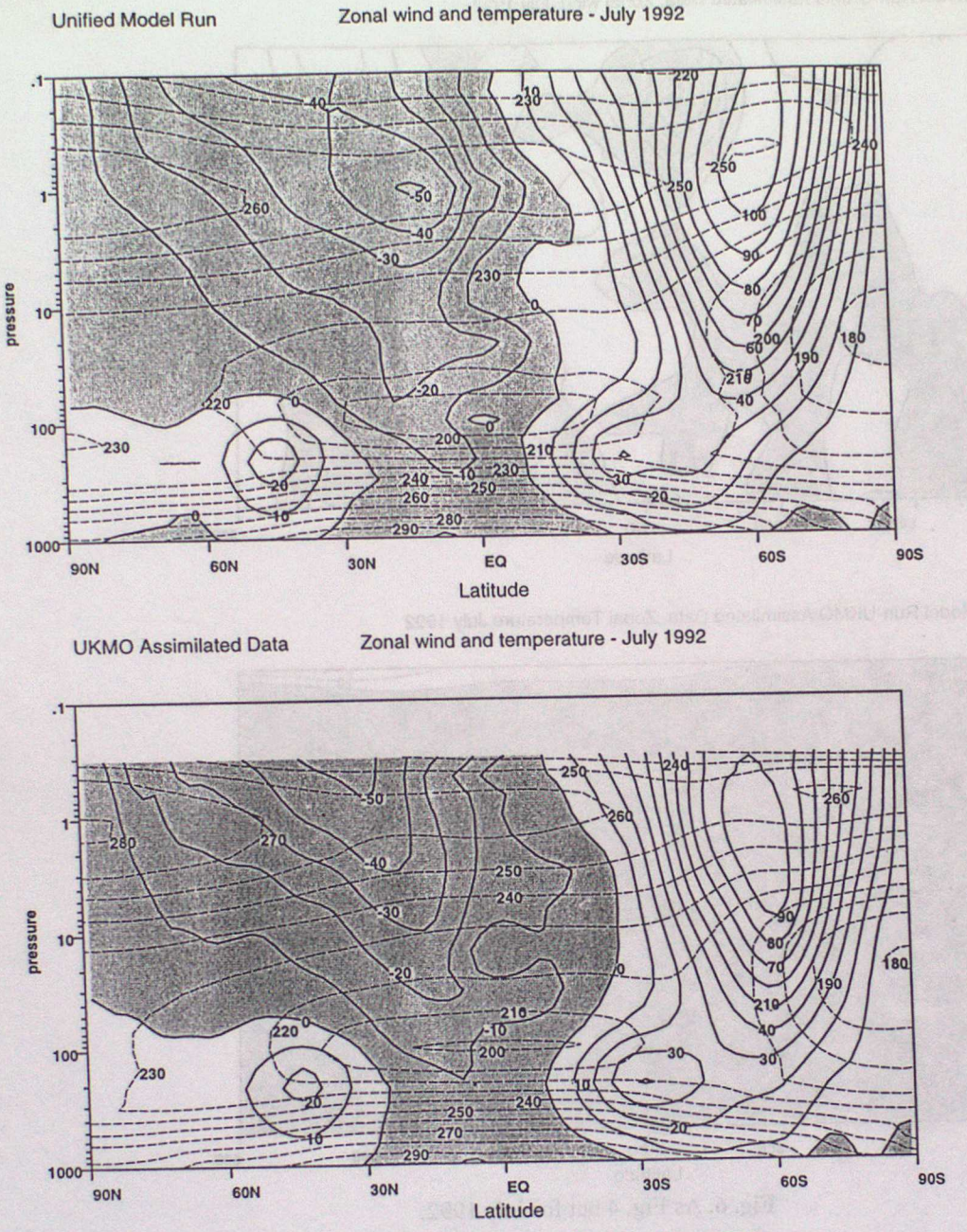

Fig. 5. As Fig. 3 but for July 1992

clearly attributed to model errors.

The subtropical jets in the UM for July 1992 were roughly similar in magnitude and shape to those in the UKMO analyses. In the northern (summer) hemisphere stratosphere, the pattern and magnitude of the easterlies in the UM was also similar to those in the UKMO analyses.

In July both the UM and the analyses had easterlies throughout the tropical stratosphere, although the UM winds were stronger. Both the QBO and the SAO were in an easterly phase during July 1992. As we saw in January, the UM has a tendency to retain easterly winds in the tropics; thus, as only about 3 months of the UM experiment (which had been initialized when the QBO was in an easterly phase) had run by July 1992, the agreement of both datasets in

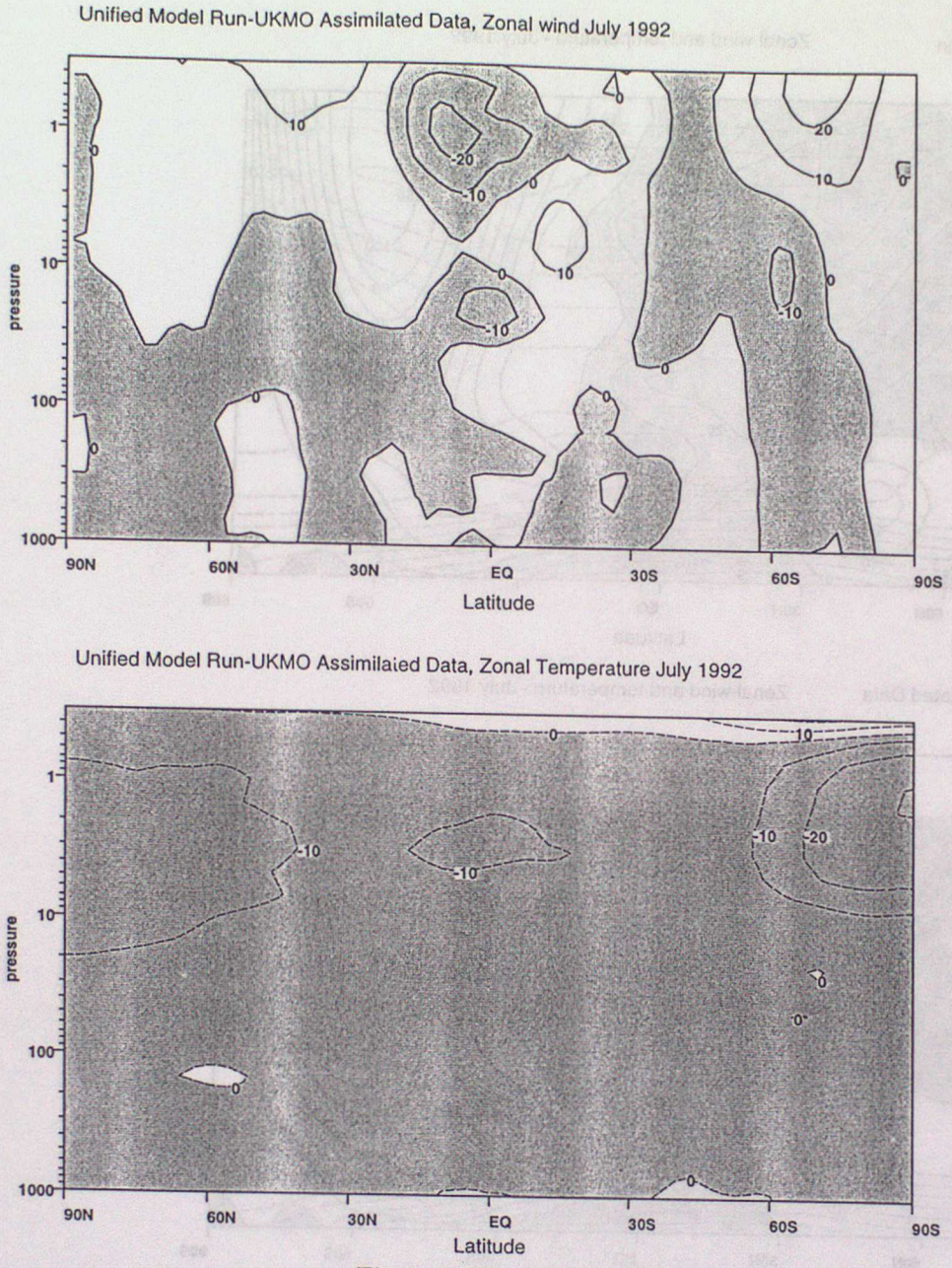

Fig. 6. As Fig. 4 but for July 1992.

capturing the easterly phase of the zonal wind in the tropics is somewhat spurious.

Figure 7 shows the monthly zonal mean (latitude versus pressure) of zonal wind and temperature for April 1993 for the UM (top panel) and the UKMO analysis (bottom panel). In both hemispheres, the shape and magnitude of the subtropical jet and the polar night jet in the UM and the UKMO analysis agree well. The early development of the southern polar vortex in the UM was similar to that in the UKMO analysis, and in both datasets the subtropical jet and the polar night jet were well separated in the northern hemisphere. Unlike January 1993 or July 1992, when the polar night jet in the UKMO analysis showed an equatorward tilt with height, the polar night jet in the UKMO analysis did not show such a tilt in April 1993. Like January 1993 and July 1992, the UM polar night jet in April 1993 did not show an equatorward tilt

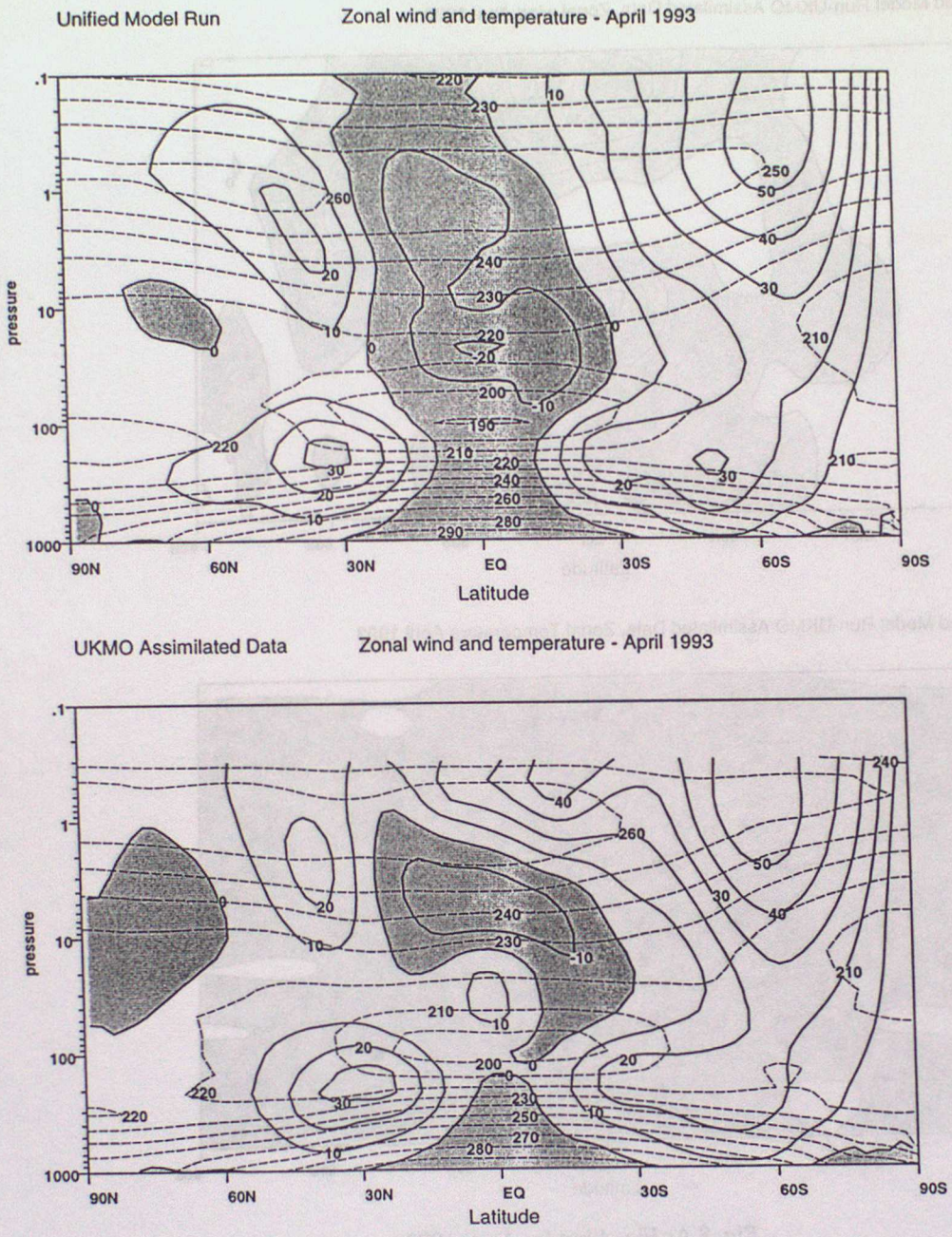

Fig. 7. As Fig. 3 but for April 1993.

with height.

The difference cross-sections (Figure 8) show that the UM is once again colder than the analyses practically everywhere. Through most of the model domain the differences are small, but in the upper stratosphere, the UM is around 10 K too cool. Since these cross-sections are from equinox, rather than solstice, seasons there is less latitudinal variation in the temperature errors, and correspondingly smaller wind differences in the extra-tropics. The most significant wind differences were in the tropics.The QBO was in a westerly phase during April 1993, with westerly winds in the lower stratosphere and easterly winds in the middle stratosphere, but the UM did not simulate the westerlies. The SAO was also in a westerly phase during April 1993, as is normal for the equinoxes. Although the UM showed a significant SAO at around 1 hPa

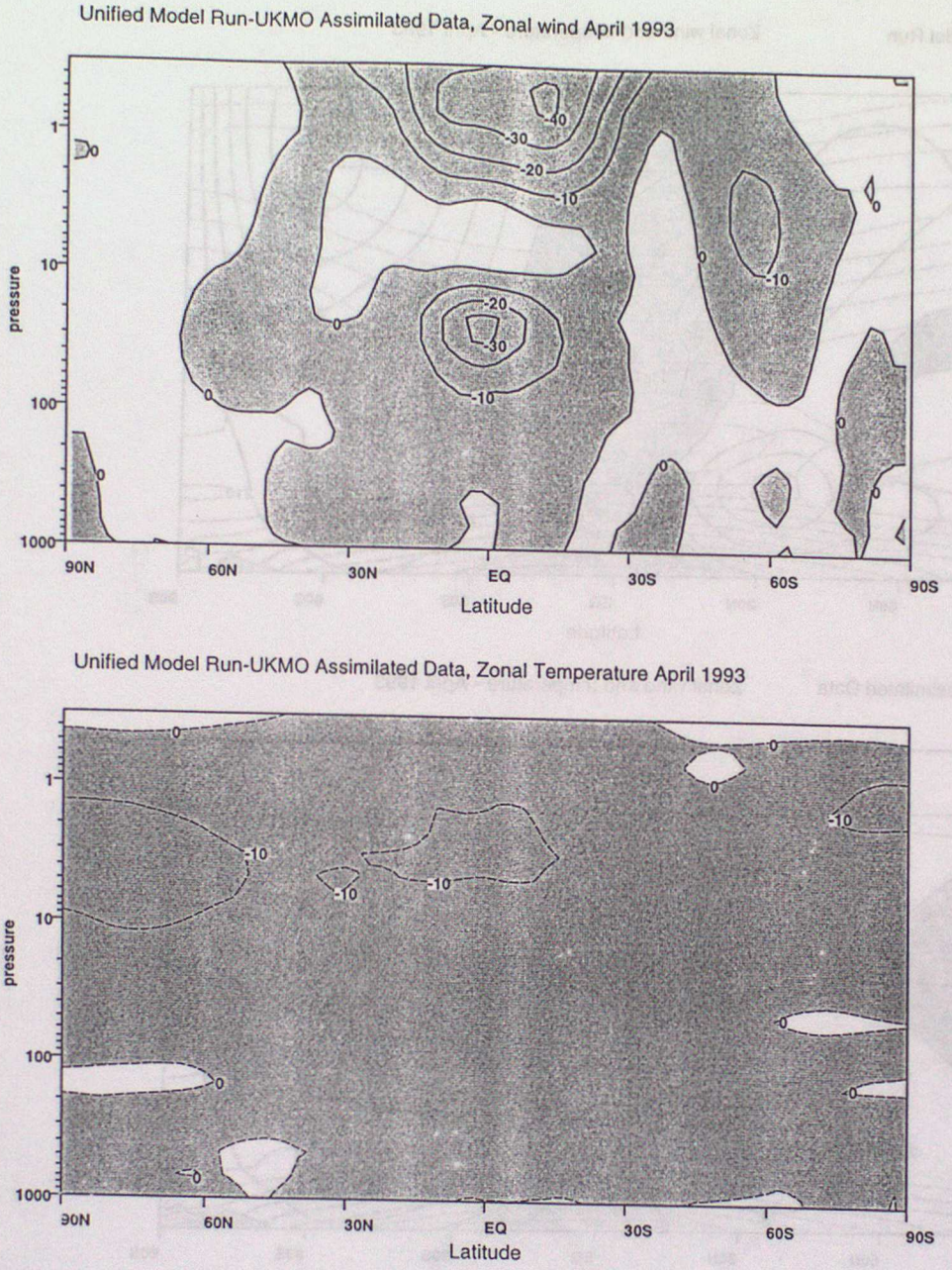

Fig. 8. As Fig. 4 but for April 1993.

over the equator, the oscillation did not involve a reversal of the winds (which were easterly).

Figure 9 shows the monthly zonal mean cross-section of zonal wind and temperature for October 1992 for the UM (top panel) and the UKMO analysis (bottom panel). The early development of the northern polar vortex is too rapid in the UM and the break-up of the southern polar vortex happens too late in the UM. As a result the stratospheric jets were too strong and deep in both hemispheres. The UM had maximum values of about 50 m/s in both hemispheres, whereas the UKMO analysis had maximum values of about 40 m/s in the northern hemisphere and about 30 m/s in the southern hemisphere.

The wind and temperature difference cross-sections for October 1992 are shown in Figure 10.

The stronger southern hemisphere jet is clearly evident. Consistent with this strong jet, the UM simulation had low temperatures in the middle stratosphere over the South Pole. Away from the South Pole, there is a cold bias of around 10 K in the upper stratosphere. In the tropics and sub-tropics there are some significant wind differences. In the northern hemisphere the UM upper tropospheric subtropical jet was closed and stronger than in the UKMO analyses, whereas the upper stratosphere westerlies were weaker than analysed. As seen in previous months, the UM does not capture the QBO westerlies in the stratosphere. The UM simulation had an SAO at around 1 hPa over the equator, but the oscillation did not show a reversal of the winds (which were easterly).

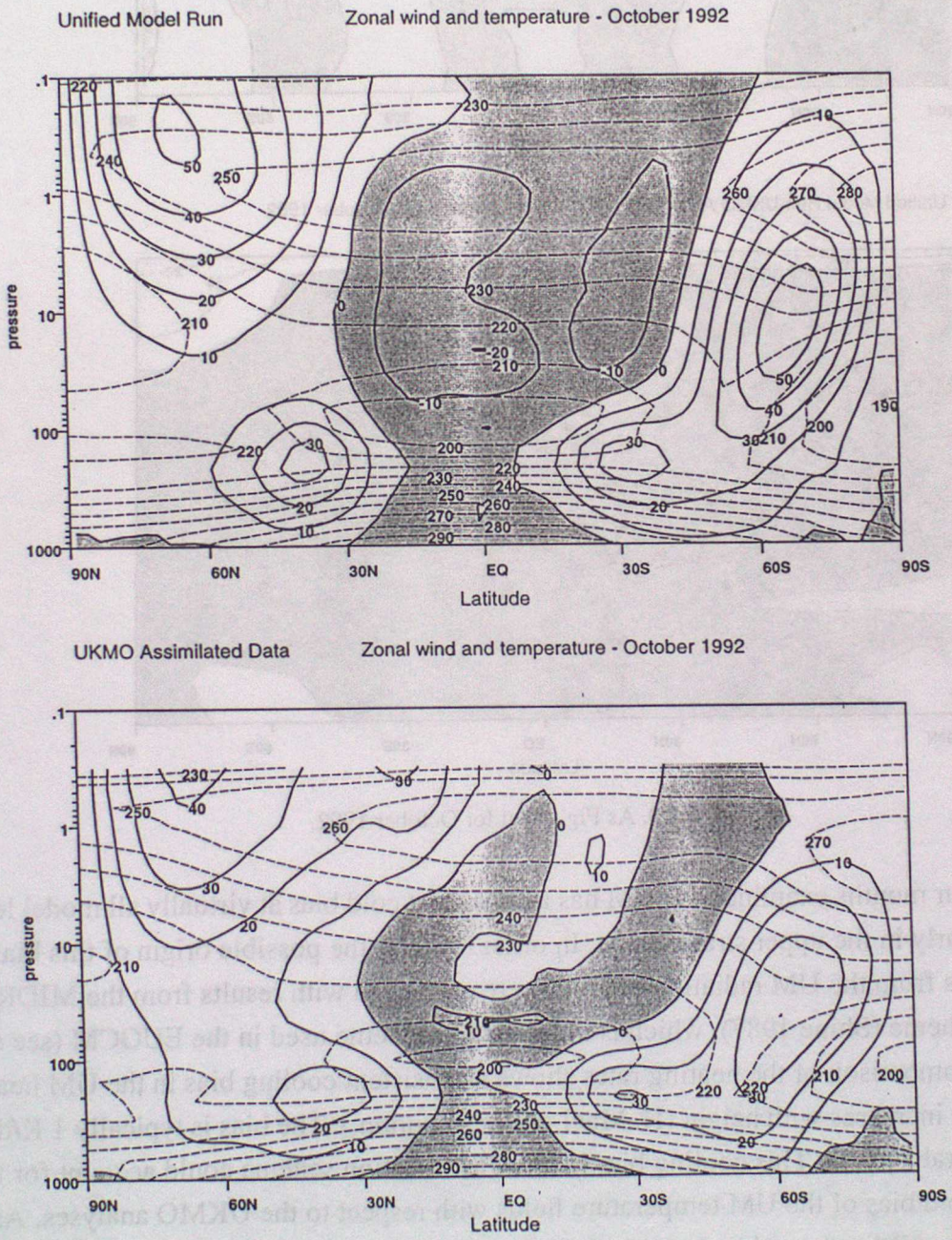

Fig. 9. As Fig. 3 but for October 1992.

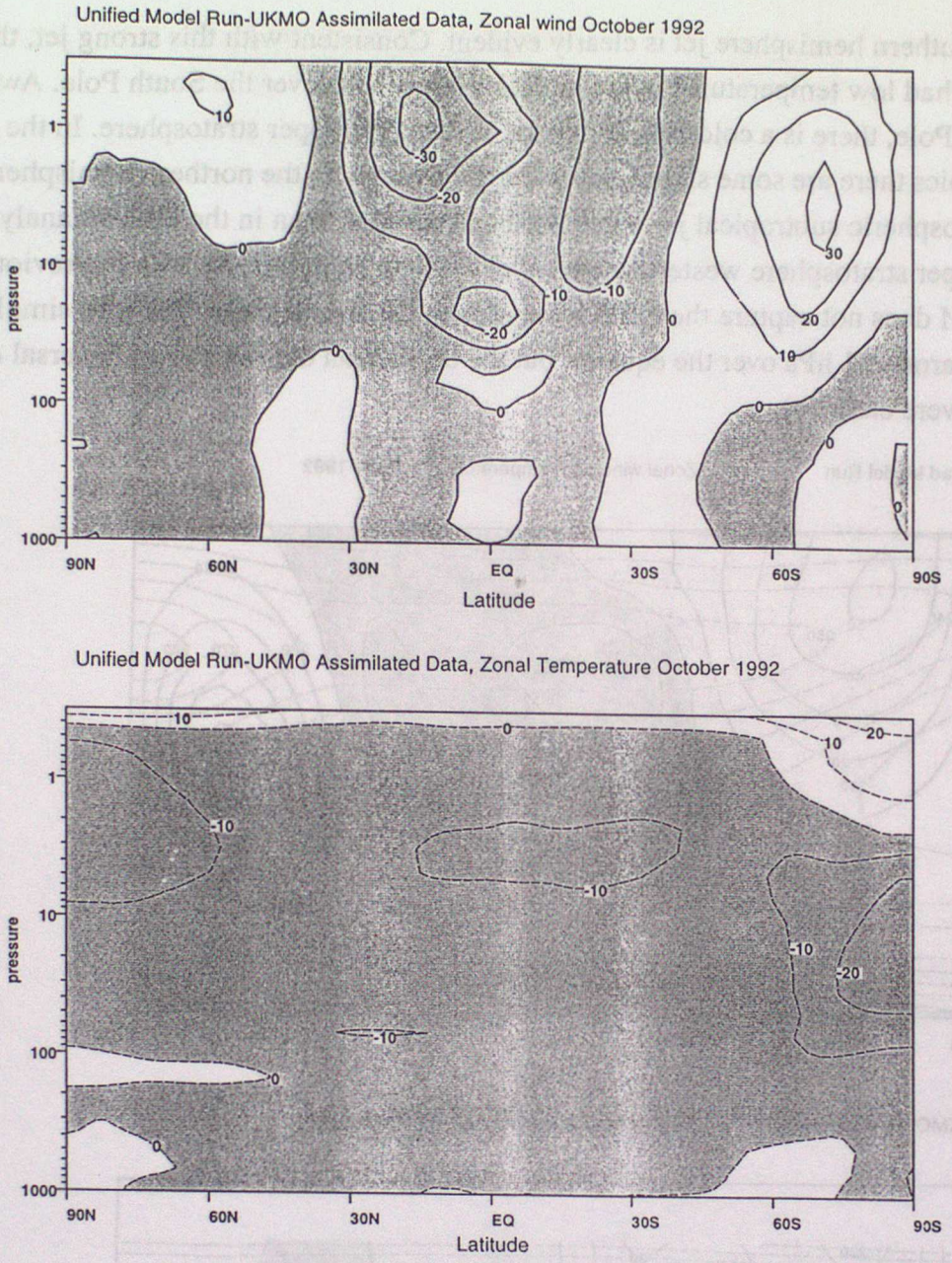

Fig. 10. As Fig. 4 but for October 1992.

In all the four months examined the UM has a consistent cold bias at virtually all model levels, but particularly in the upper stratosphere. In order to study the possible origin of this bias, heating rates from the UM radiation scheme were compared with results from the MIDRAD radiation scheme (Shine 1987), which is the radiation scheme used in the EUGCM (see section 3.3). Comparison of the heating rates shows a consistent cooling bias in the UM heating rates, which increases with height (H. MacLean pers. comm.). The bias is typically 1 K/day in the upper stratosphere. This cooling bias in the UM radiation scheme could account for the generally cold bias of the UM temperature fields with respect to the UKMO analyses. As a version of the UM was used in deriving the UKMO analyses (see section 3.2), this model bias may also account for the slight cool bias in the UKMO analyses near 10 hPa, as compared to other stratospheric analyses (see, for example, Swinbank and O'Neill 1994, or Coy and Swin-

bank 1996).

Figures 11 and 12 show time series of zonal wind and temperature, respectively, for the UM (top panel) and the UKMO analyses (bottom panel). The plots are shown at three levels: 100 hPa (Figures 11a and 12a), 10 hPa (b) and 1 hPa (c). Although differences between the UM and the UKMO analysis will arise through interannual variability, this is a fair comparison in the sense that both datasets have the same time-span and none of them is the average of a longer time-span.

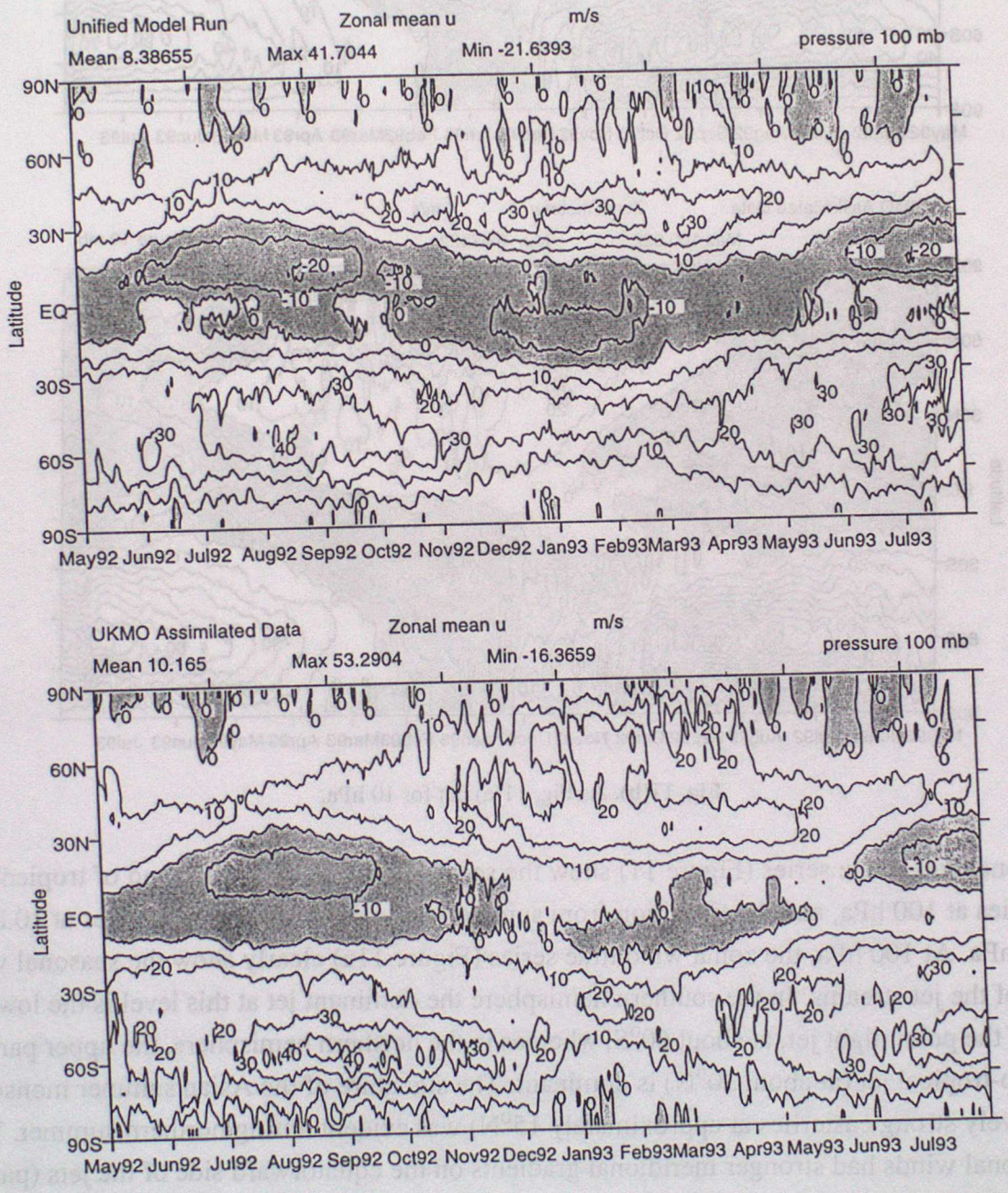

Fig. 11(a). Time series (time v latitude) of UM zonal wind (m/s -- top panel) and UKMO analysis zonal wind (m/s -- bottom panel) for the period of the run (May 1992-July 1993) at 100 hPa. The shading indicates easterly winds (negative values of the zonal wind).

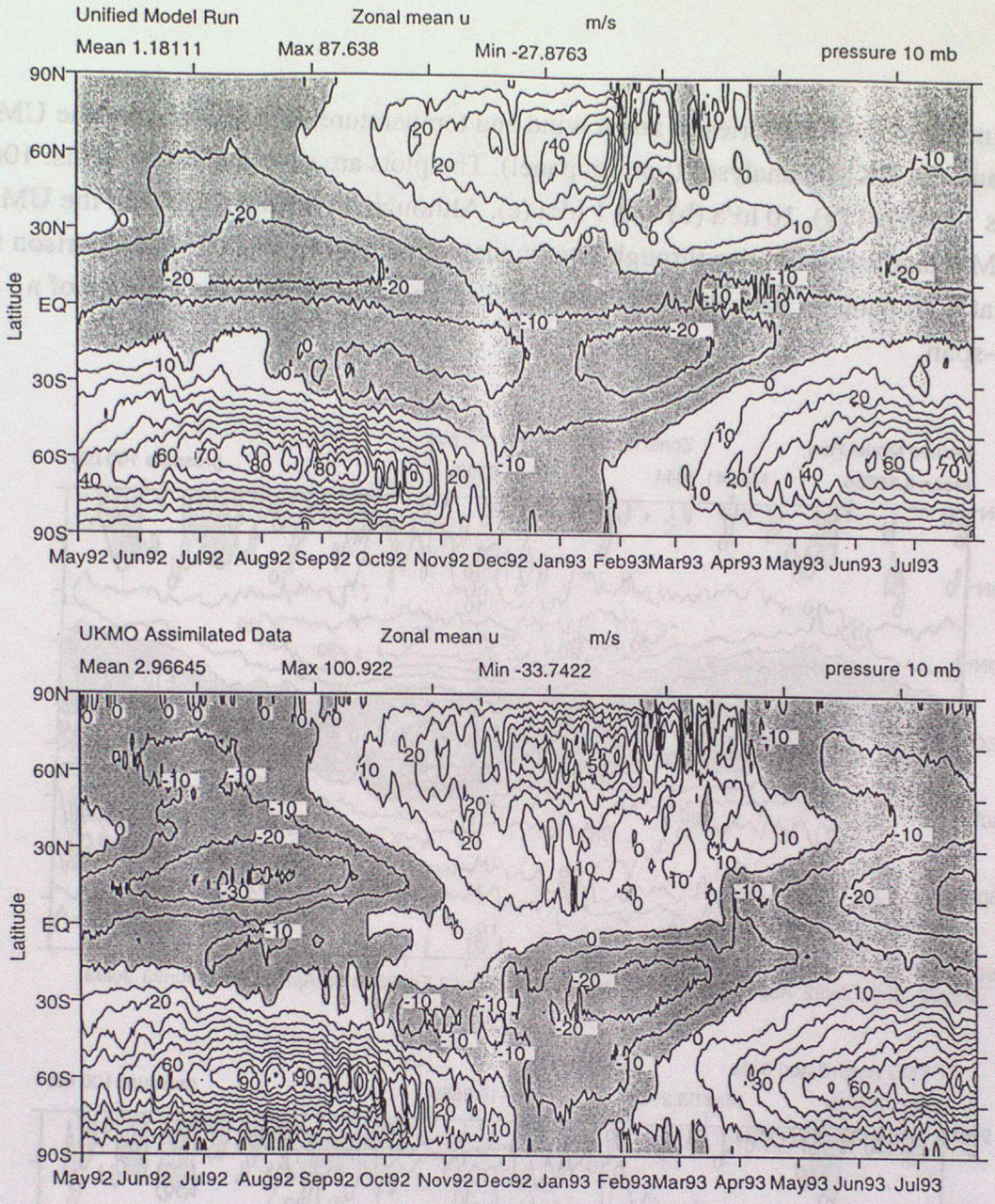

Fig. 11(b). As Fig. 11(a) but for 10 hPa.

The zonal wind time series (Figure 11) show the seasonal migration of the band of tropical easterlies at 100 hPa, and the transition from summer easterlies to winter westerlies at 10 hPa and 1 hPa. At 100 hPa, the zonal wind time series (Figure 11a) clearly show the seasonal variation of the jet streams. In the southern hemisphere the dominant jet at this level is the lower part of the polar night jet, at about 60°S, whereas in the northern hemisphere, the upper part of the sub-tropical jet (at about 30°N) is dominant. The signature of the Asian summer monsoon (relatively strong easterlies at approximately 15°N) was evident during northern summer. The UM zonal winds had stronger meridional gradients on the equatorward side of the jets (particularly in the northern hemisphere). In the tropics, the UM winds were significantly more easterly than in the UKMO analyses.

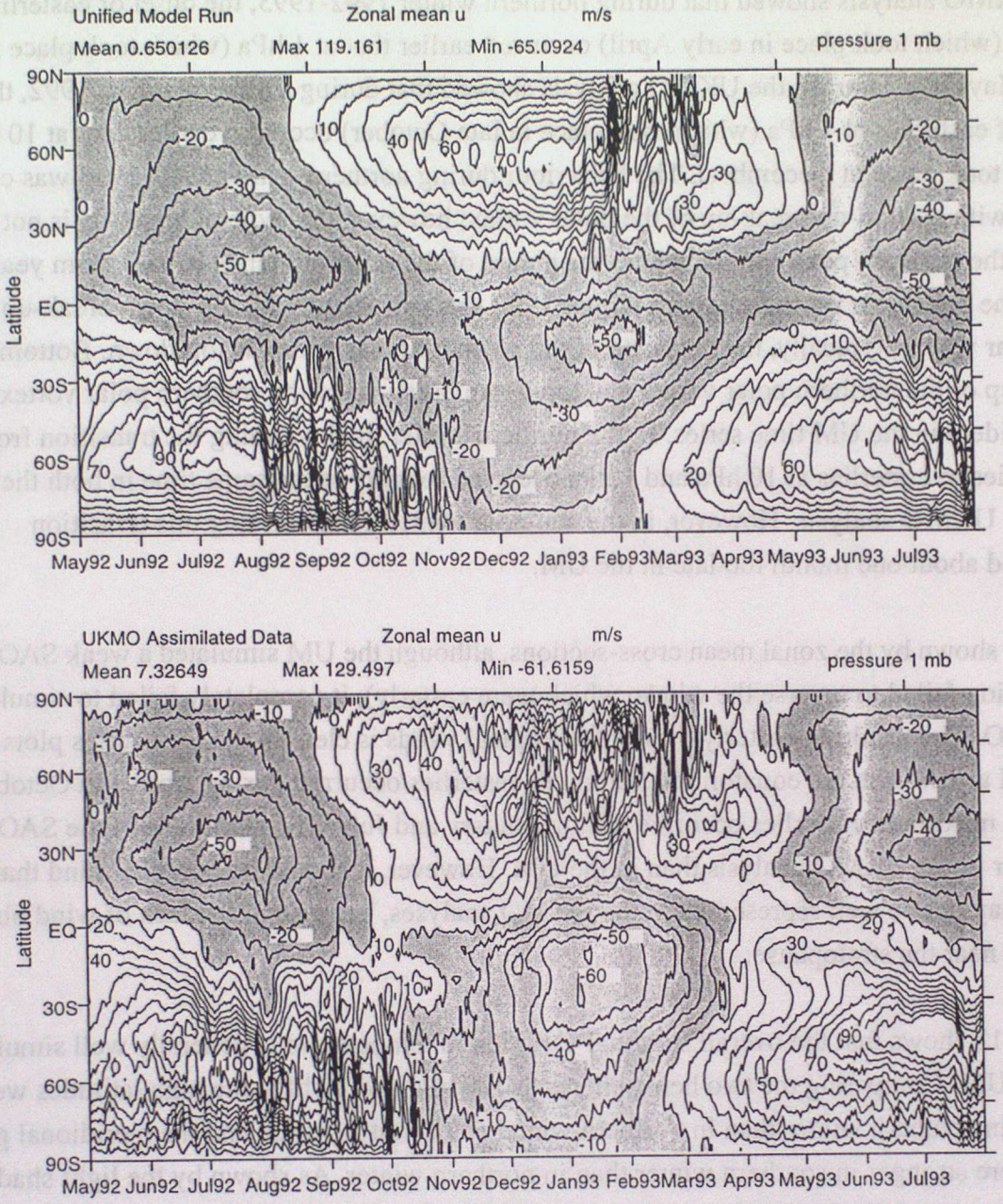

Fig. 11(c). As Fig. 11(a) but for 1 hPa.

At 10 hPa and 1 hPa (Figures 11b and c) the maximum values in the wintertime westerly jets are similar in the UKMO analysis and in the UM (typical values being about 100 m/s). The meridional gradients on the equatorward flank of the wintertime jets were similar in the UM and the UKMO analysis; however, on the poleward flank of the wintertime jets, the UM had less high frequency variability than the UKMO analysis. These plots also highlight the difference between the two hemispheres in the UM simulation; at both 10 hPa and 1 hPa the jet was some 30 m/s stronger in southern winter than in northern winter. Both the UM and the UKMO analysis showed warmings during the 1992-1993 northern winter; note the wind reversals at both 10 hPa and 1 hPa in late winter. However, the spatial and temporal extent of the warmings was slightly larger in the UM.

The UKMO analysis showed that during northern winter 1992-1993, the onset of easterlies at 10 hPa (which took place in early April) occurred earlier that at 1 hPa (which took place in early May). By contrast, the UKMO analysis showed that during southern winter 1992, the onset of easterlies at 1 hPa (which took place in late October) occurred earlier than at 10 hPa (which took place in December). The behaviour during northern winter 1992-1993 was consistent with bottom-up break-up of the polar vortex; however, this type of break-up is not typical for the northern polar vortex, where the nature of the break-up tends to vary from year to year. The behaviour during southern winter 1992 was consistent with top-down break-up of the polar vortex; typically, the break-up of the southern polar vortex is top-down. Bottom-up break-up of the northern polar vortex and top-down break-up of the southern polar vortex was also evident in the UM time series. In the northern winter final warming the transition from westerlies to easterlies at 10 hPa and 1 hPa occurred roughly at the same time in both the UM and the UKMO analysis. However, in the southern winter final warming this transition occurred about one month too late in the UM.

As was shown by the zonal mean cross-sections, although the UM simulated a weak SAO (the oscillation failed to reverse the winds, which were easterly), it completely failed to simulate the QBO. The resulting easterly bias in the tropical winds is clear in the time series plots. In the UM at 1 hPa on the equator, the minimum easterlies occurred during April and October and the maximum easterlies occurred during January and July. The amplitude of the SAO was stronger in the UKMO analysis than in the UM. However, it should be borne in mind that the SAO may not be well represented in the UKMO analyses, because of the lack of wind observations near the stratopause.

Figure 12 shows that the overall seasonal variation in temperature is generally well simulated by the UM. Comparing the two hemispheres at 100 hPa and 10 hPa, the high latitudes were colder in southern winter than in northern winter (by about 5-10 K), and the meridional gradients were stronger in southern winter than in northern winter. As shown by the light shading on the upper panels, the UM results were generally colder than the UKMO analyses (typically by about 5-10 K in the mid to upper stratosphere). At 10 hPa and 1 hPa, the high latitude temperatures varied relatively smoothly through early winter. In late winter the UM simulation showed strong warming pulses at 10 hPa and at 1 hPa (e.g. during February and March 1993, and during October 1992), which were in good qualitative agreement with the analyses. In the tropics, where temporal variability is low, the differences between the UM and the UKMO analysis are more significant, while at high winter latitudes these differences are affected by both interannual and short time-scale variability.

Both the UKMO analysis and the UM had weak warming pulses in early northern winter 1992-1993 at 10 hPa and 1 hPa (see Figures 11-12); however, the UM showed less temporal variability than the UKMO analysis. Synoptic maps of geopotential height show that the UM had a weak Canadian warming (see, e.g. Juckes and O'Neill 1988) in mid November 1992.

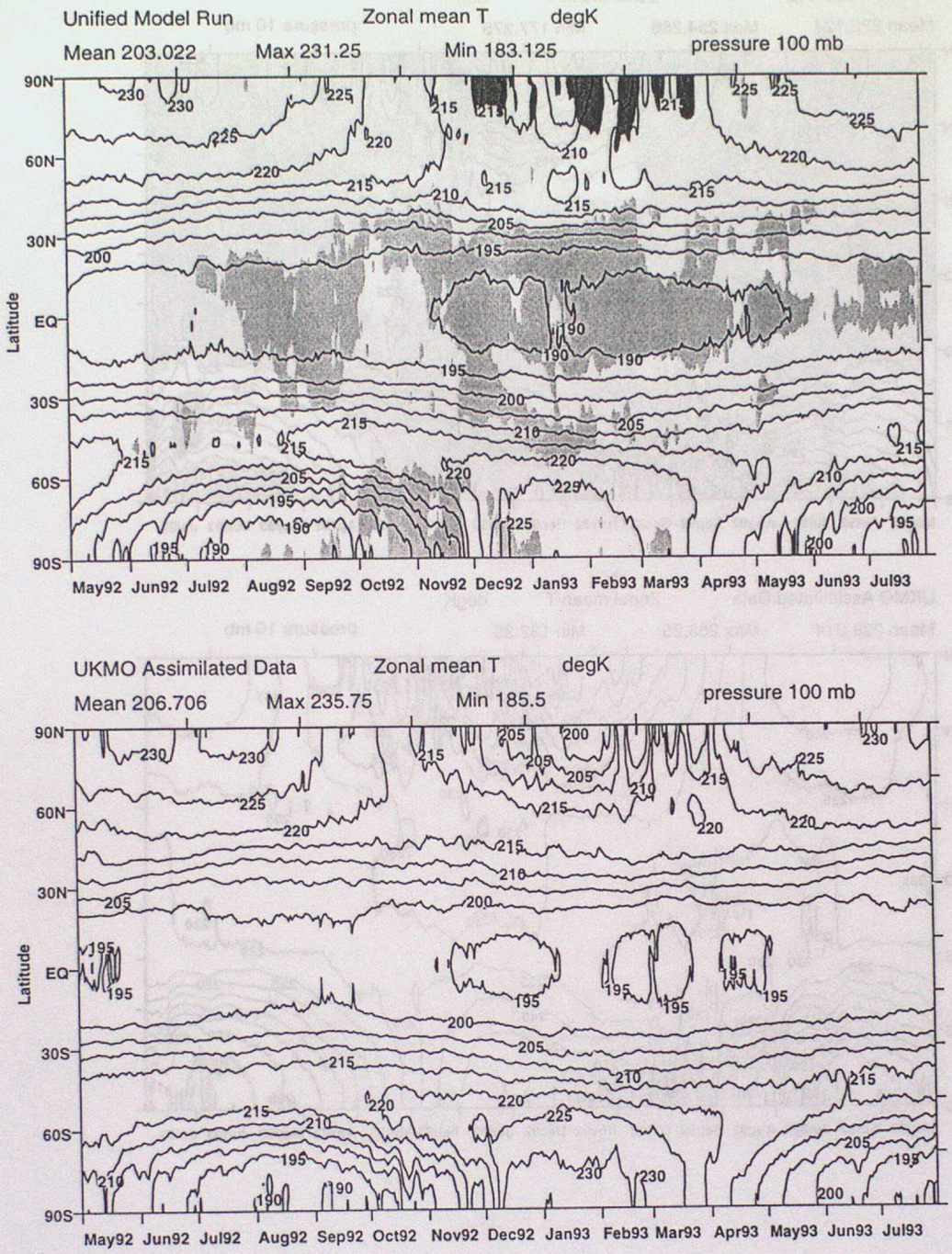

Fig. 12(a). As Fig. 11 but for UM temperature (K -- top panel) and UKMO analysis temperature (K -- bottom panel) for 100 hPa. The unshaded area in the UM time series indicates where the UM and the UKMO analysis differ by less than 5 K; the lightly shaded area indicates where the UM is more than 5 K colder than the UKMO analysis; the heavily shaded area indicates where the UM is more than 5 K warmer than the UKMO analysis.

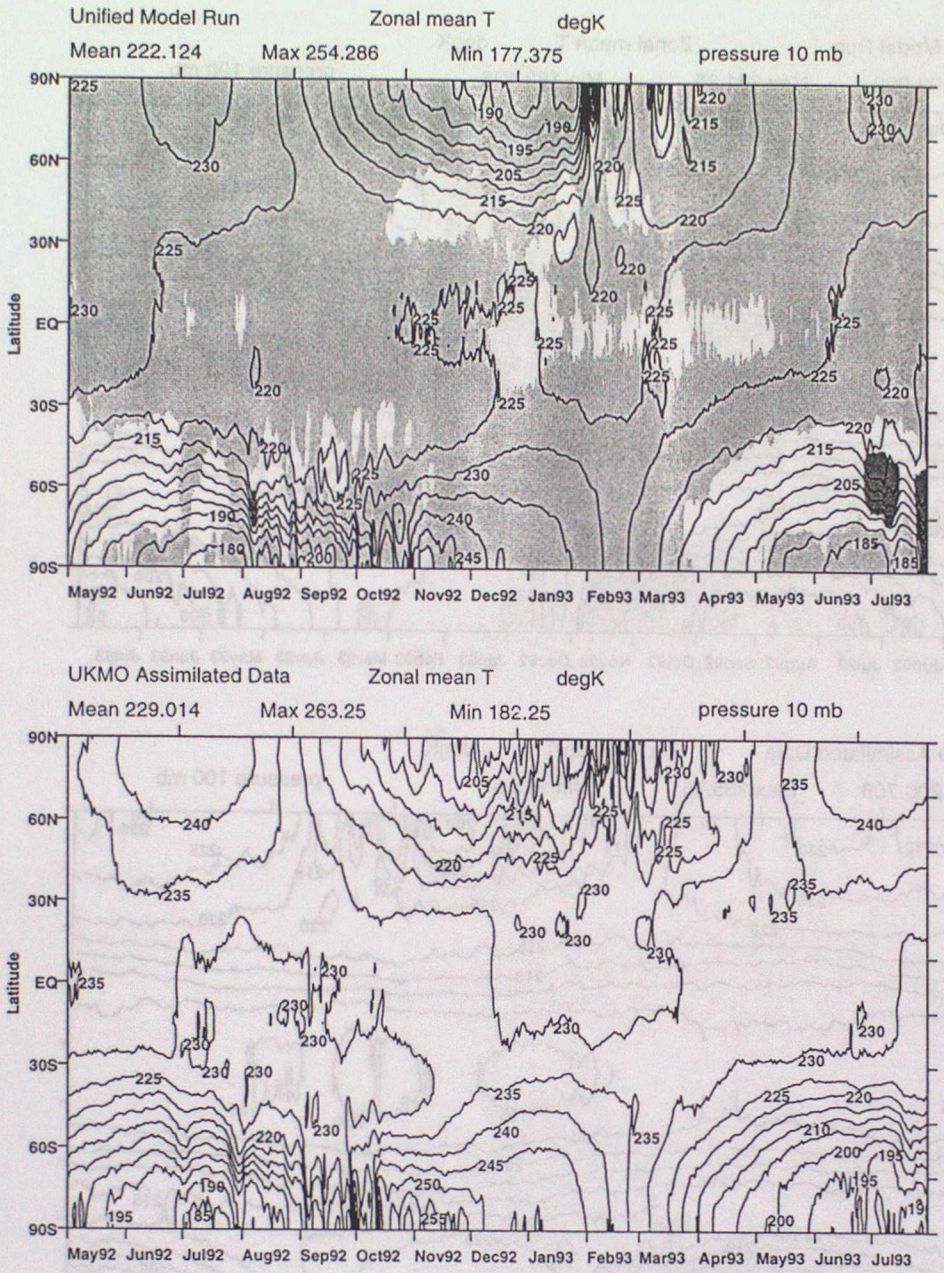

Fig. 12(b). As Fig. 12(a) but for 10 hPa.

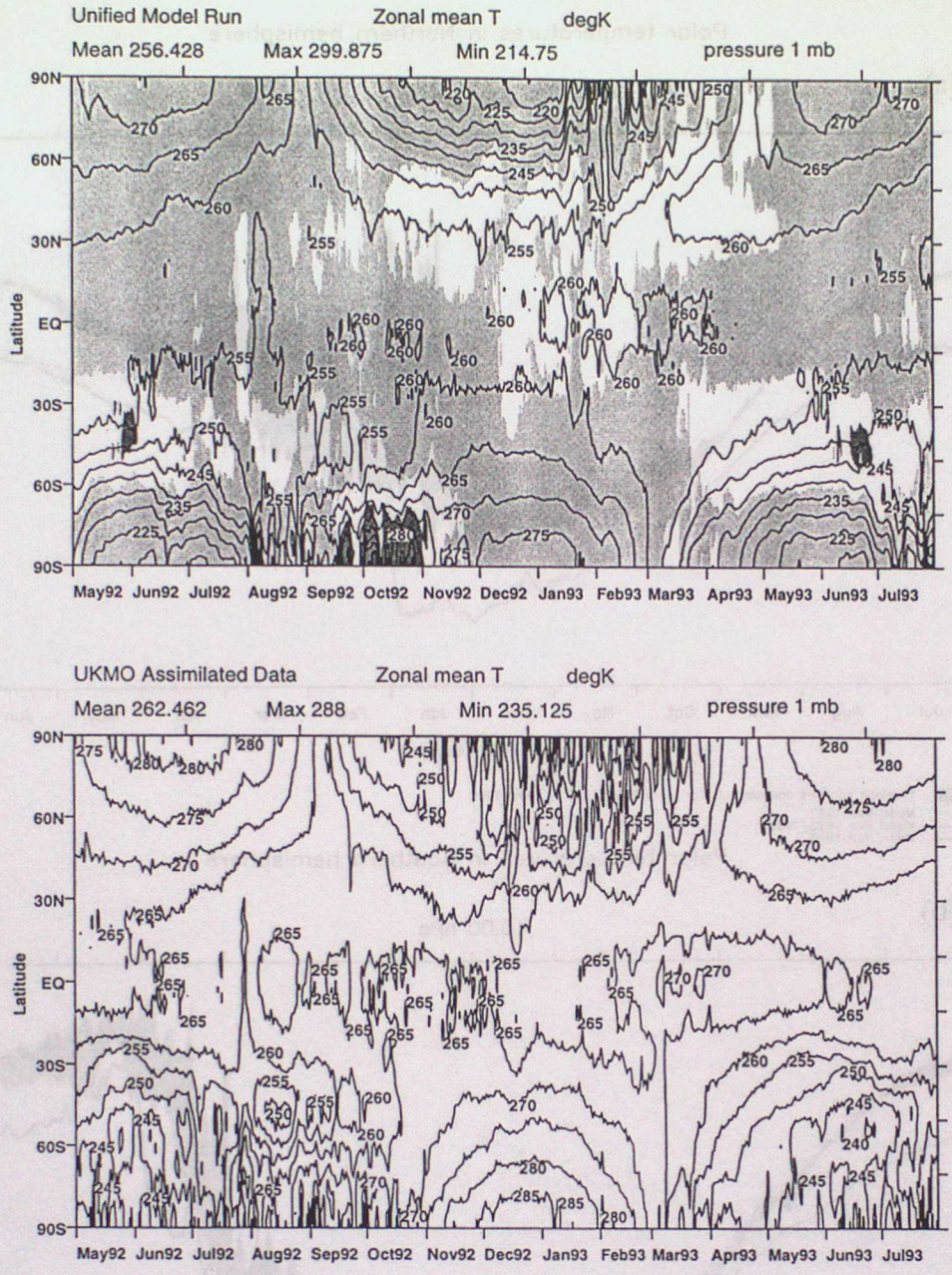

Fig. 12(c). As Fig. 12(a) but for 1 hPa.

4.2 Stratospheric Warmings

Figure 13 shows a time series of the simulated 10 hPa temperature over the North Pole (Figure 13a) and South Pole (Figure 13b) for the model run. The grey shading is the envelope containing UKMO analysis temperature time series for different years. The UM had a cold bias of about 15 K at the North Pole, except during the period February to March 1993, when two warmings occurred: in the first one the temperature rose by about 60 K in a few days; in the second one it rose by about 15 K over a similar period. The UM also had a cold bias of about 5-10 K at the South Pole. The South Pole time series showed no large sudden warmings, but the temperature warmed gradually during middle and late winter 1992 and during July 1993. There were occasional bursts of short time-scale temperature rises (of order 5-10 K)

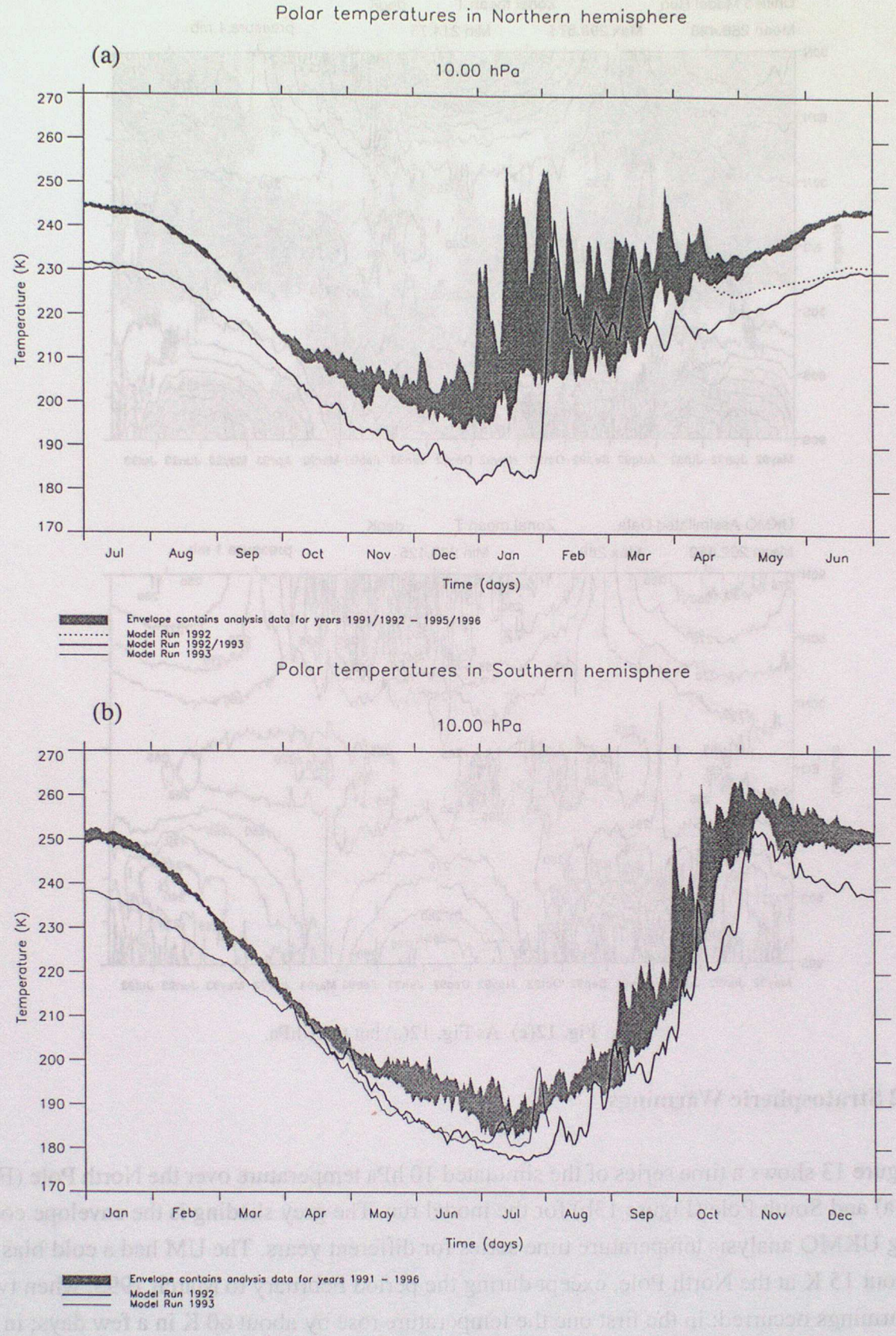

Fig. 13. Polar temperatures at 10 hPa in the UM for: (a) the northern hemisphere; (b) the southern hemisphere. The gray shading in (a) is the envelope of several years (1991-1992, 1992-1993, 1993-1994, 1994-1995, 1995-1996) of 10 hPa north pole temperatures from the UKMO analysis. The gray shading in (b) is the envelope of several years (1991, 1992, 1993, 1994, 1995, 1996) of 10 hPa south pole temperatures from the UKMO analysis.

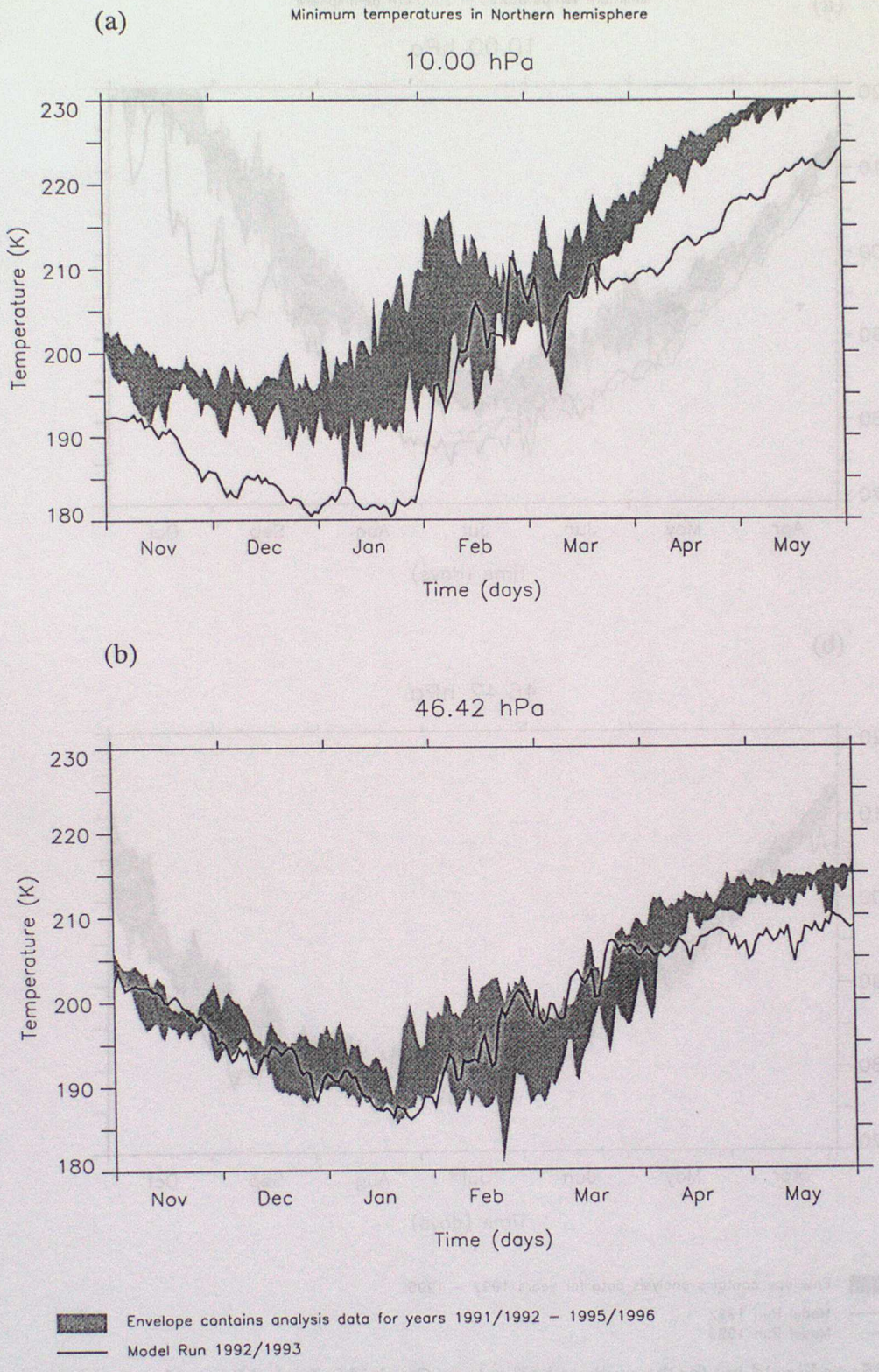

Fig. 14. Minimum temperature in the UM for the northern hemisphere at (a) 10 hPa; (b) 46 hPa. Overlaid in (a) and (b) are the envelopes of several years of UKMO analysis temperatures: 1991-1992, 1992-1993, 1993-1994, 1994-1995, 1995-1996.

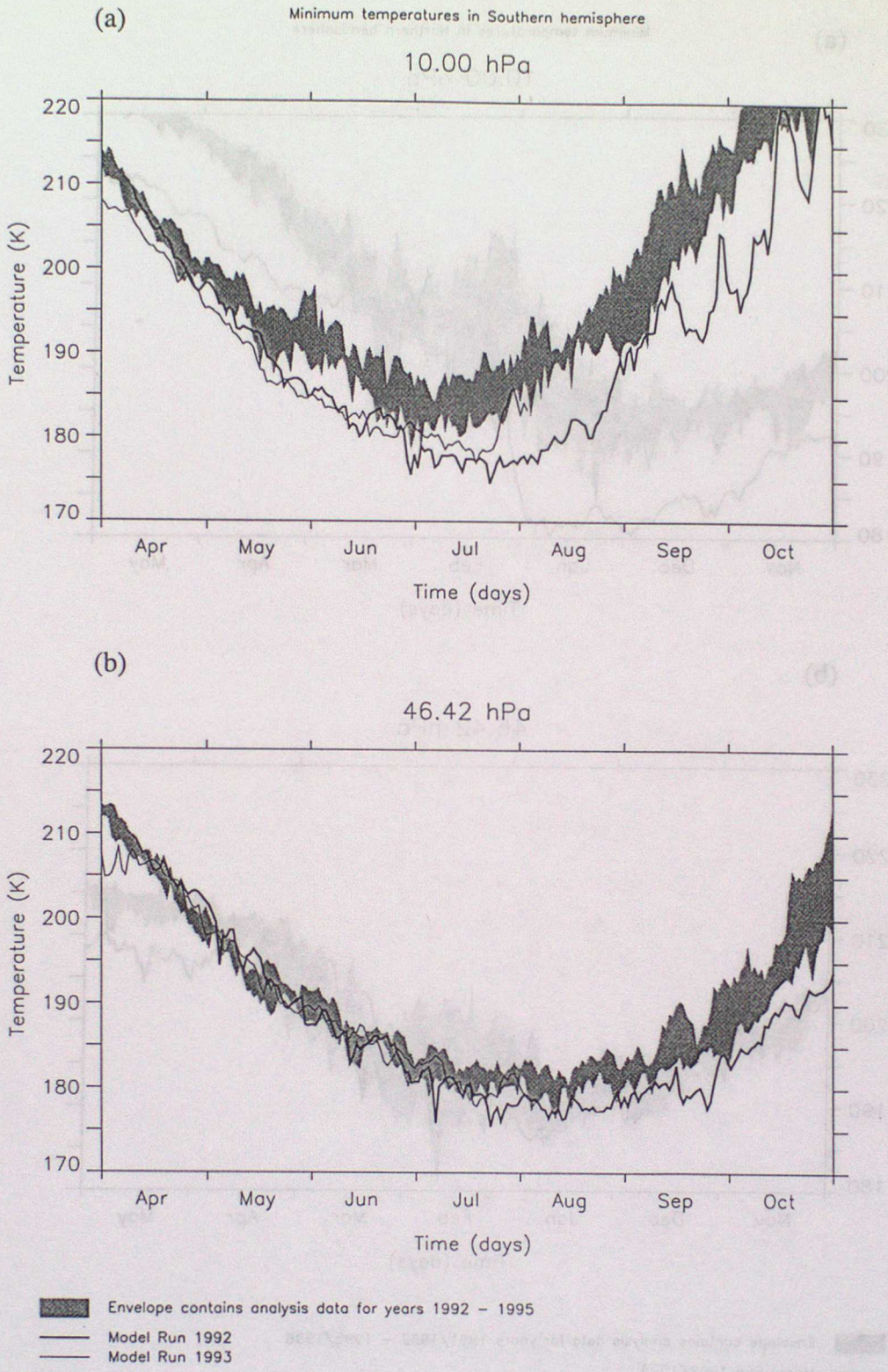

Fig. 15. As Fig. 14 but for the southern hemisphere. Overlaid in (a) and (b) are the envelopes of several years of UKMO analysis temperatures: 1992, 1993, 1994, 1995.

superimposed on the slowly increasing temperatures. Figures 14 and 15 show the evolution of the UM minimum temperature at 46 hPa and 10 hPa for the northern hemisphere and southern hemisphere, respectively. The warmings which occurred during February to March 1993 are evident in the minimum northern hemisphere temperatures at both 46 hPa and at 10 hPa,

although the signal at 46 hPa is much weaker. The southern hemisphere time series (Figure 15) show the general warming which occurred during the late southern winter of 1992. The temperature increase occurs earlier at 10 hPa than at 46 hPa, consistent with top-down break-up of the southern polar vortex.

Figure 16 (geopotential heights at 10 hPa) shows the development of the January 1993-February 1993 warming in the UM. On 28 January (Figure 16a), the polar vortex was well-developed and slightly displaced off the pole, and a tongue from it was being pulled around the

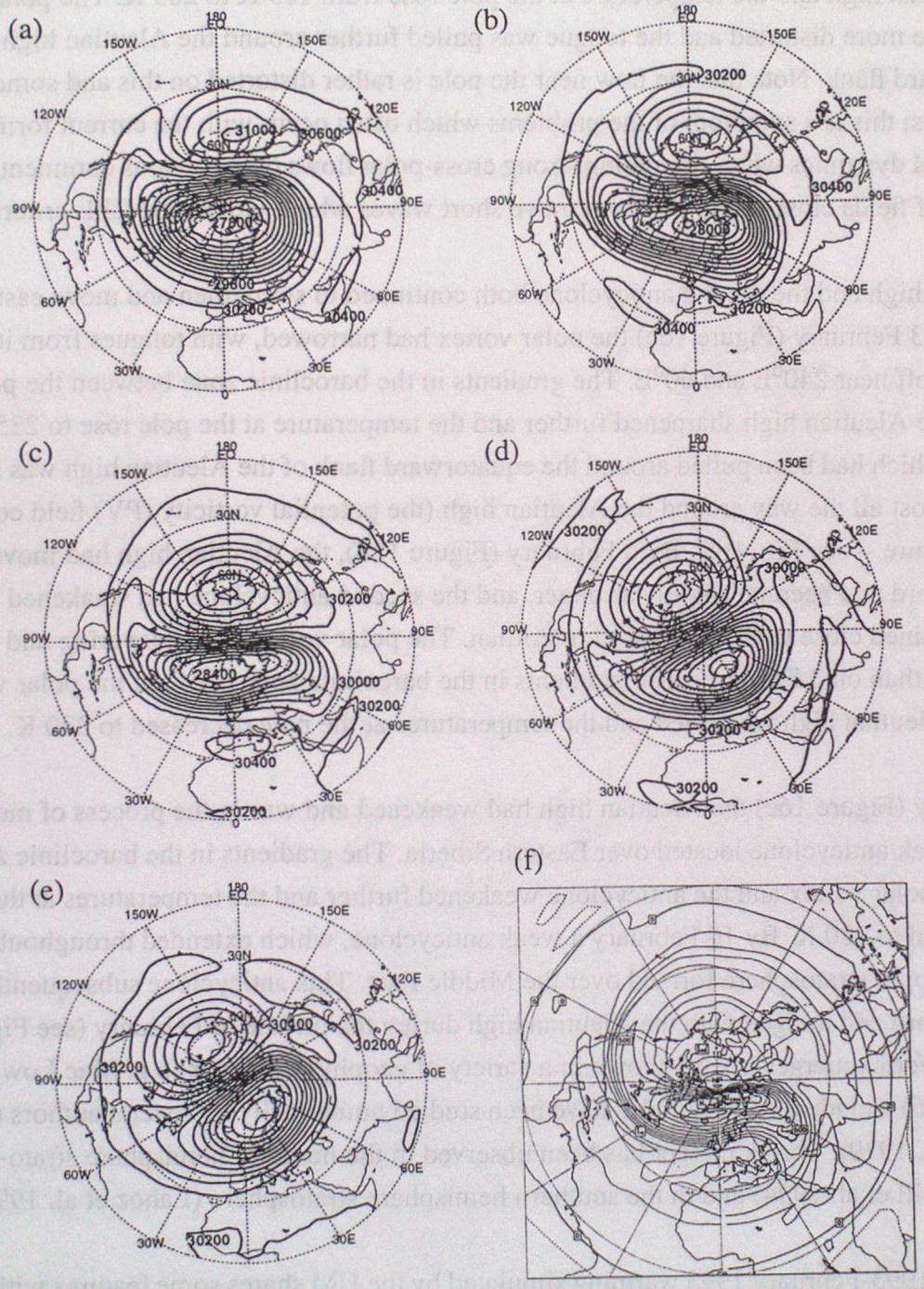

Fig. 16. Synoptic maps of UM 10 hPa geopotential height (m) fields (contour interval 200 m) for: (a) 28 January 1993; (b) 31 January 1993; (c) 3 February 1993; (d) 6 February 1993; (e) 9 February 1993; (f) synoptic map of 840 K potential vorticity (PV) (PV units) for 3 February 1993.

eastern flank of a strong anticyclone located over the dateline. This anticyclone (the Aleutian high), and the warm pool of air associated with it, extended throughout the middle and upper stratosphere and tilted westward with height. The vertical extent and westward tilt with height of this anticyclone persisted throughout the period of the warming.

By 31 January (Figure 16b) the Aleutian high had strengthened and a second anticyclone formed over 330°E. The gradients sharpened in the baroclinic zone between the polar vortex and the Aleutian high and the temperature at the pole rose from 185 K to 205 K. The polar vortex became more distorted and the tongue was pulled further around the Aleutian high to the equatorward flank. Note that the flow near the pole is rather distorted on this and some of the other maps; this is a symptom of the problems which often occur with the current formulation of the UM dynamics when simulating strong cross-polar flows (see previous comments on the filtering of fields close to the pole to remove short waves which violate the CFL criterion).

The Aleutian high and the second anticyclone both continued to strengthen and move eastward, and by 3 February (Figure 16c) the polar vortex had narrowed, with tongues from it being pulled off near 240°E and 60°E. The gradients in the baroclinic zone between the polar vortex and the Aleutian high sharpened further and the temperature at the pole rose to 235 K. The tongue which had been pulled around the equatorward flank of the Aleutian high was now stretched almost all the way around the Aleutian high (the potential vorticity (PV) field confirms this picture -- see Fig. 16f). By 6 February (Figure 16d), the Aleutian high had moved further eastward and become slightly stronger, and the second anticyclone had weakened further and remained close to the Greenwich meridian. The polar vortex was recovering and was less distorted than on 3 February. The gradients in the baroclinic zone between the polar vortex and the Aleutian high weakened and the temperatures at the pole decreased to 230 K.

By 9 February (Figure 16e) the Aleutian high had weakened and was in the process of merging with a weak anticyclone located over Eastern Siberia. The gradients in the baroclinic zone between the polar vortex and the anticyclone weakened further and the temperatures at the pole decreased to 220 K. By 10 February a weak anticyclone, which extended throughout the middle and upper stratosphere formed over the Middle East. This anticyclone subsequently moved eastward and merged with the Aleutian high during the middle of February (see Figure 17a below). Vortex merger is well known in a variety of geophysical flows (e.g. Mac Low and Ingersoll 1986) and idealized examples have been studied numerically by several authors (e.g. Zabusky et al. 1979). Vortex merger has been observed in the northern hemisphere stratosphere (O'Neill et al. 1994) and in the southern hemisphere stratosphere (Lahoz et al. 1996).

The January 1993-February 1993 warming simulated by the UM shares some features with the stratospheric warming which occurred during mid January 1992 and was documented by O'Neill et al. (1994). Both warmings showed a tongue of air from the polar vortex being

drawn around the Aleutian high in the middle stratosphere. In both cases this was followed by interaction between the Aleutian high and an eastward travelling anticyclone. The interaction between these vortices led to the distortion and weakening of the polar vortex.

Figure 17 shows a sequence of geopotential height maps at 10 hPa (left-hand column) and 1 hPa (right-hand column), to illustrate the subsequent synoptic evolution in the northern hemisphere winter, including the final warming. On 14 February (Figure 17a) the stratospheric polar vortex was disturbed at both 10 hPa and 1 hPa and there was a strong anticyclone at 10 hPa. As mentioned previously, the anticyclone at 10 hPa was split into two unequal parts, which subsequently merged. At 1 hPa the strengths of the two anticyclones were reversed, with a weak anticyclone located over the date line and a strong anticyclone located over the Mediterranean.

By 26 February (Figure 17b) the polar vortex had weakened. At 10 hPa there was a strong quasi-stationary anticyclone located over the date line which did not reach to the 1 hPa level, and a weak eastward travelling anticyclone located over the North Atlantic. At 10 hPa the polar vortex was squeezed between these two anticyclones and was shifted slightly off the pole. At 1 hPa the vortex was more extensive, with strong gradients between the vortex centre and an anticyclone which was located over Northern Europe and extended down to the 10 hPa level. At 1 hPa the vortex extended well into Eastern Asia, and had strong gradients on its southern-most flank in that region.

By 10 March (Figure 17c) the quasi-stationary anticyclone had intensified and a weak eastward travelling anticyclone had developed over the North Atlantic; at 1 hPa the polar vortex remained strong but was in the process of being split into two by an anticyclone located over Eastern Europe. Over the next few days the polar vortex split and then recovered. Between mid March and mid April (Figures 17d-f) the polar vortex continued to weaken dramatically at 10 hPa, but much more slowly at 1 hPa, consistent with a bottom-up break-up of the polar vortex in the northern winter final warming. As mentioned previously, the manner in which the northern polar vortex breaks-up differs from year to year and this bottom-up break-up is not typical.

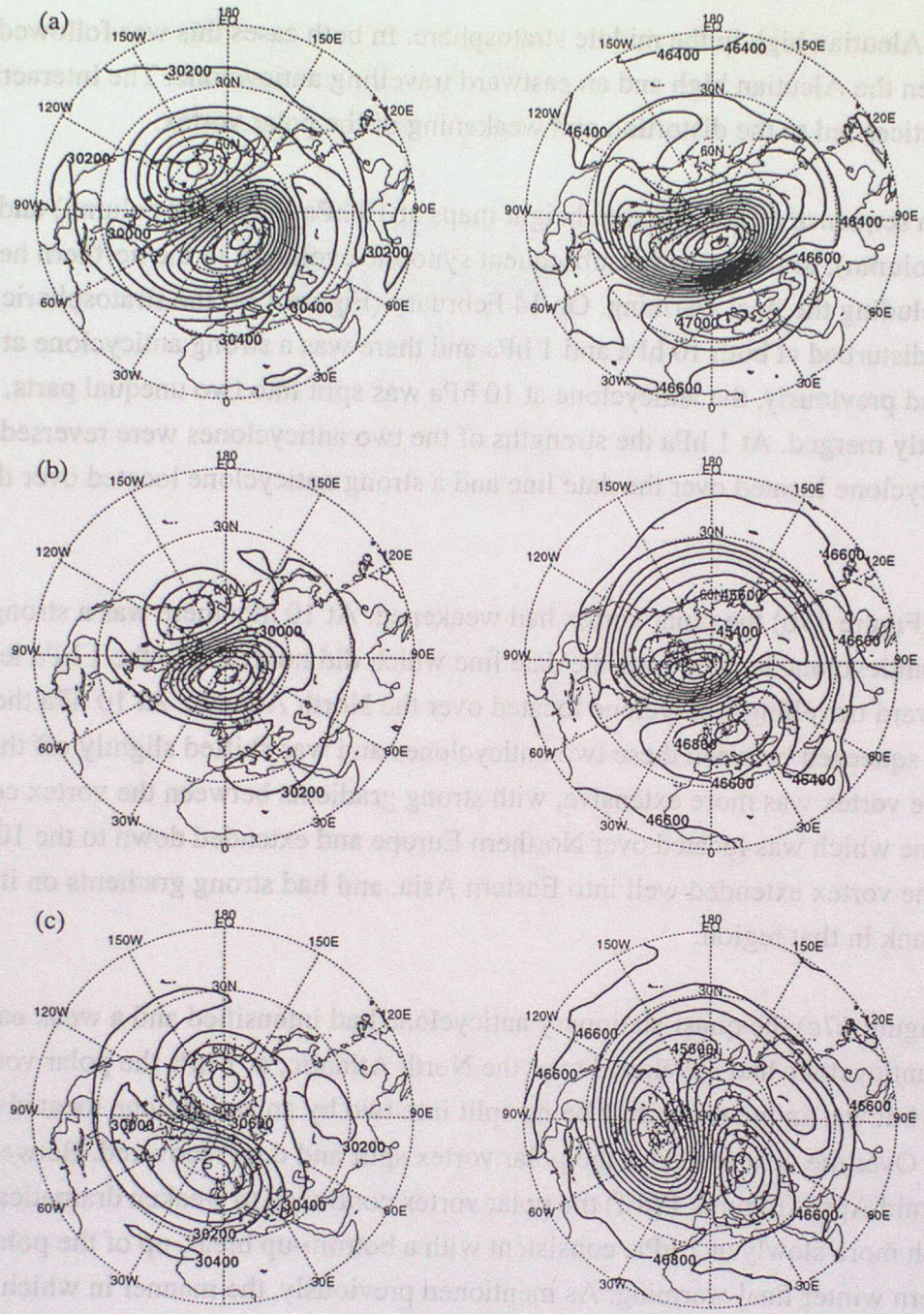

Fig. 17. Synoptic maps of UM geopotential height (m) fields at 10 hPa (left-hand panels) and 1 hPa (right-hand panels) for: (a) 14 February 1993; (b) 26 February 1993; (c) 10 March 1993

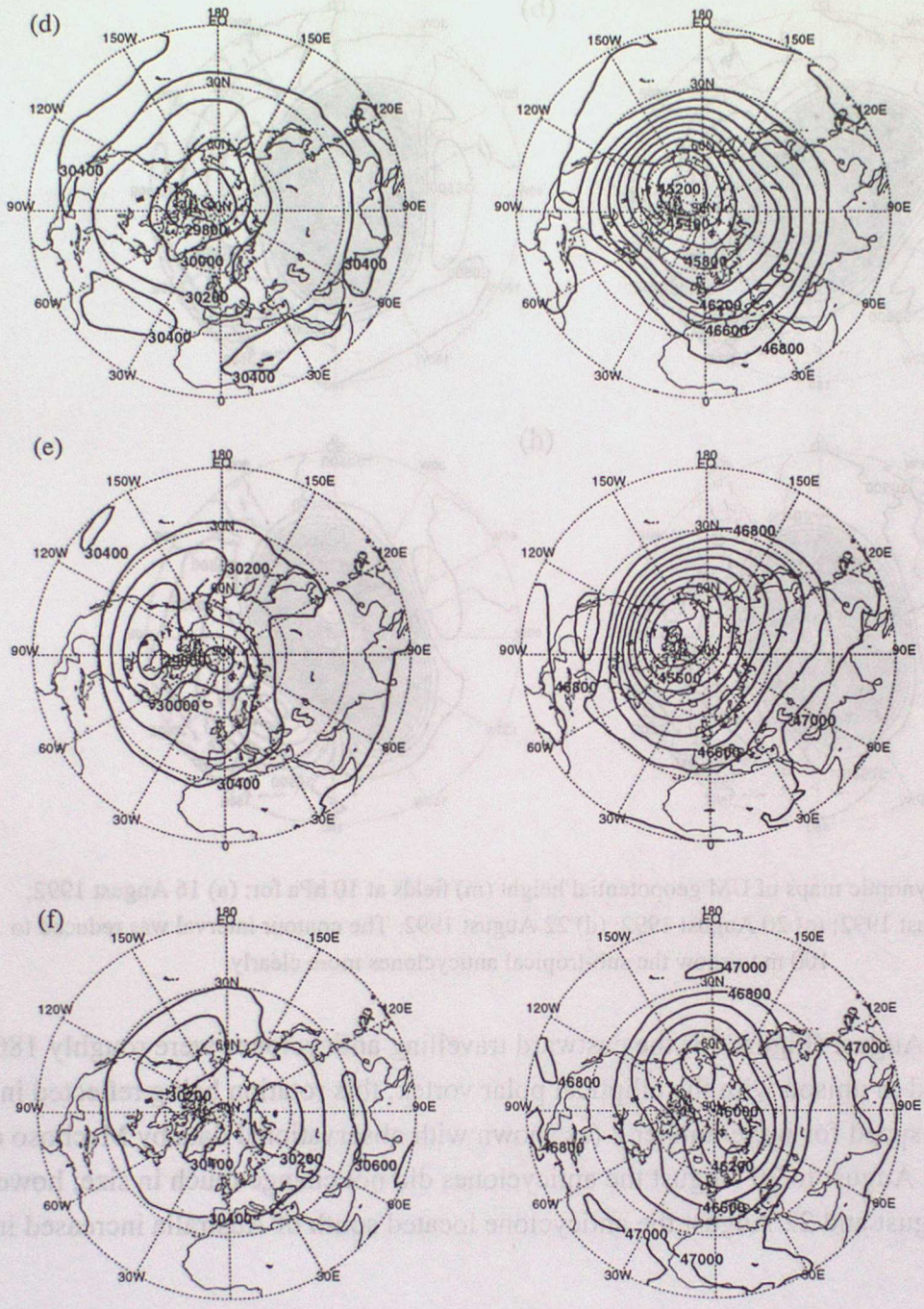

Fig. 17(cont). (d) 22 March 1993; (e) 3 April 1993; (f) 15 April 1993.

In the stratosphere of the southern hemisphere, the springtime transition from winter westerlies to summer easterlies -- the final warming -- tends to occur along similar lines each year (Mechoso et al. 1988). Commonly, the final warming is preceded by a transition from a disturbed flow regime in which developing anticyclones are advected eastward and decay to a flow regime in which an anticyclone becomes quasi-stationary over a preferred geographical location (roughly the sector 90°E to 180°E).

Figure 18 shows a sequence of geopotential height maps at 10 hPa which is typical of the synoptic evolution during the middle of the southern hemisphere winter. Over the period

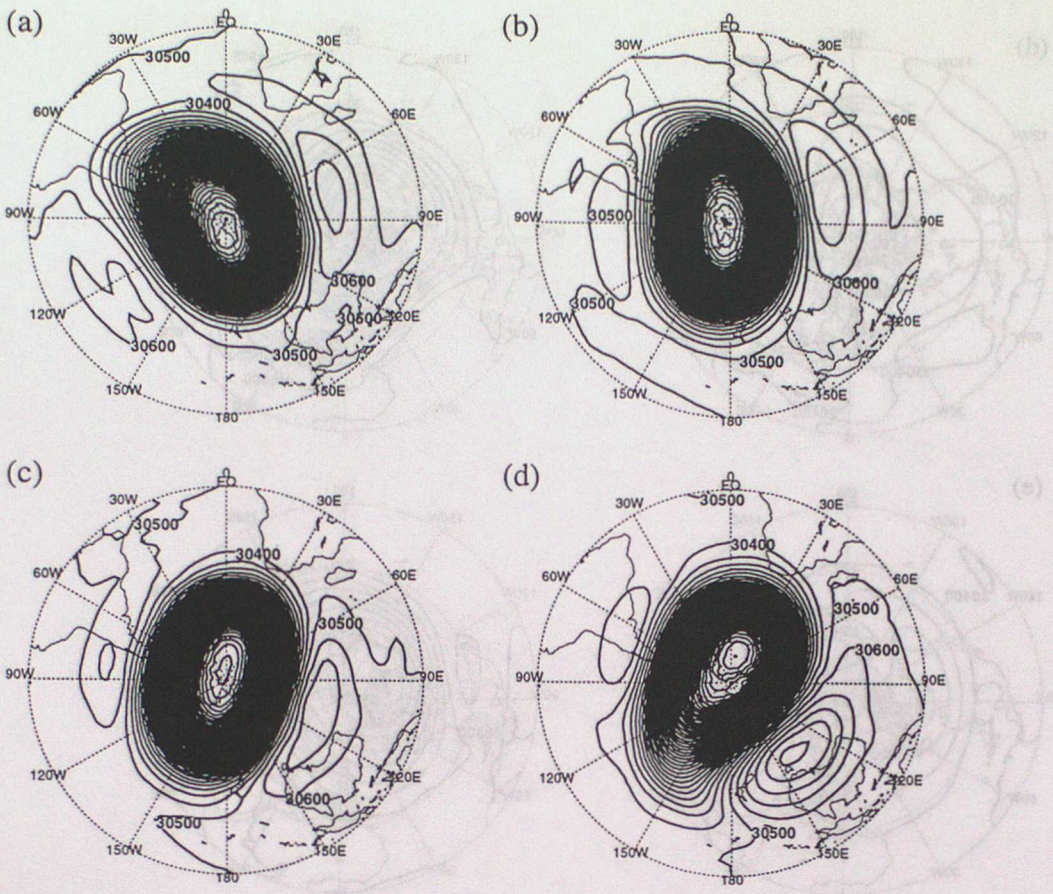

Fig. 18. Synoptic maps of UM geopotential height (m) fields at 10 hPa for: (a) 16 August 1992; (b) 18 August 1992; (c) 20 August 1992; (d) 22 August 1992. The contour interval was reduced to 100 m to show the sub-tropical anticyclones more clearly.

16 August - 22 August (Figure 18) the eastward travelling anticyclones were roughly 180° apart and rotated in unison with the elliptical polar vortex, this rotation being reflected in an eastward phase speed for wavenumber 2 (as shown with observational data by Mechoso et al. 1988). From 16 August to 20 August the anticyclones did not change much in size; however, between 20 August and 22 August the anticyclone located south of Australia increased in strength.

During the next few days the anticyclone located south of Australia slowed down over a region south of Australia and New Zealand and just west of the date line, while the second anticyclone (located over South America on 22 August) continued to move eastward. By late August the anticyclone located South of Australia on 22 August was located to the west of the date line and South of New Zealand and had become quasi-stationary, while the eastward travelling anticyclone had caught up and was merging with it. This transition from a flow regime of eastward travelling anticyclones to a flow regime in which an anticyclone becomes quasi-stationary over a preferred geographical location occurs slightly early in the UM; in particular, in southern winter 1992, there were quasi-stationary anticyclones in July and August located south of Australia.

Figure 19 shows a sequence of geopotential height maps at 10 hPa (left-hand column) and 1 hPa (right-hand column), to illustrate the subsequent synoptic evolution in the southern hemisphere winter, including the final warming. On 30 September (Figure 19a) the polar vortex was disturbed at 10 hPa and 1 hPa and two anticyclones were present at 10 hPa. One anticyclone was located south of Africa and was moving eastward, the other was located over New Zealand and was quasi-stationary. At 1 hPa the eastward travelling anticyclone was in the process of merging with the quasi-stationary anticyclone and the merger of anticyclones was pushing the polar vortex off the pole towards South Pacific mid latitudes.

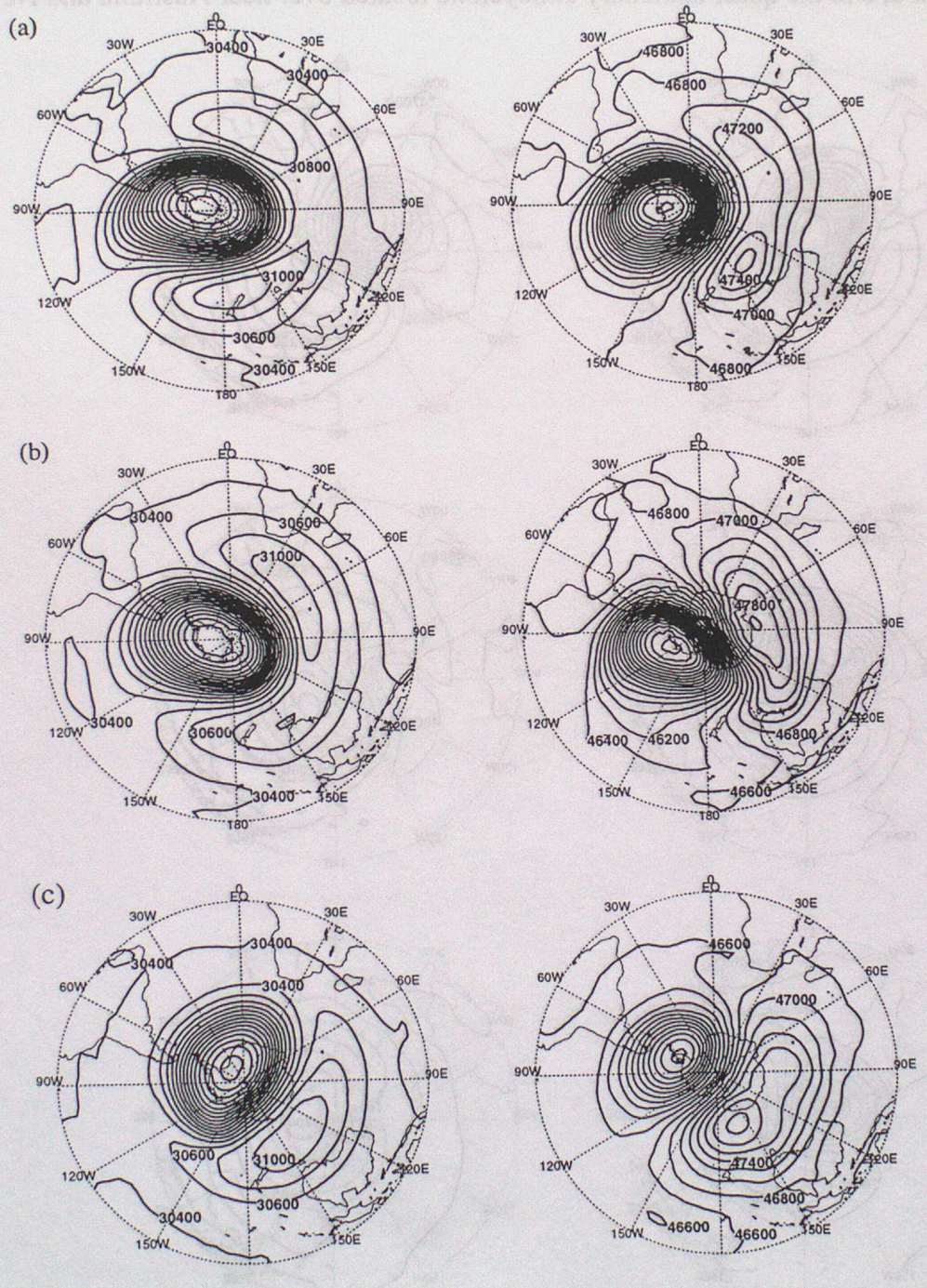

Fig. 19. Synoptic maps of UM geopotential height (m) fields at 10 hPa (left-hand panels) and 1 hPa (right-hand panels) for: (a) 30 September 1992; (b) 2 October 1992; (c) 10 October 1992;

By 2 October (Figure 19b) the two anticyclones has started to merge at 10 hPa, while at 1 hPa the merger was virtually complete, forming a large and deep anticyclone located over the southern Indian Ocean. At 1 hPa the polar vortex was more disturbed than at 10 hPa, and the baroclinic zone between the polar vortex and the anticyclones was more intense at 1 hPa than at 10 hPa.

By 10 October (Figure 19c) the polar vortex had weakened considerably at 1 hPa but only slightly at 10 hPa, and the quasi-stationary anticyclone located over near Australia and New

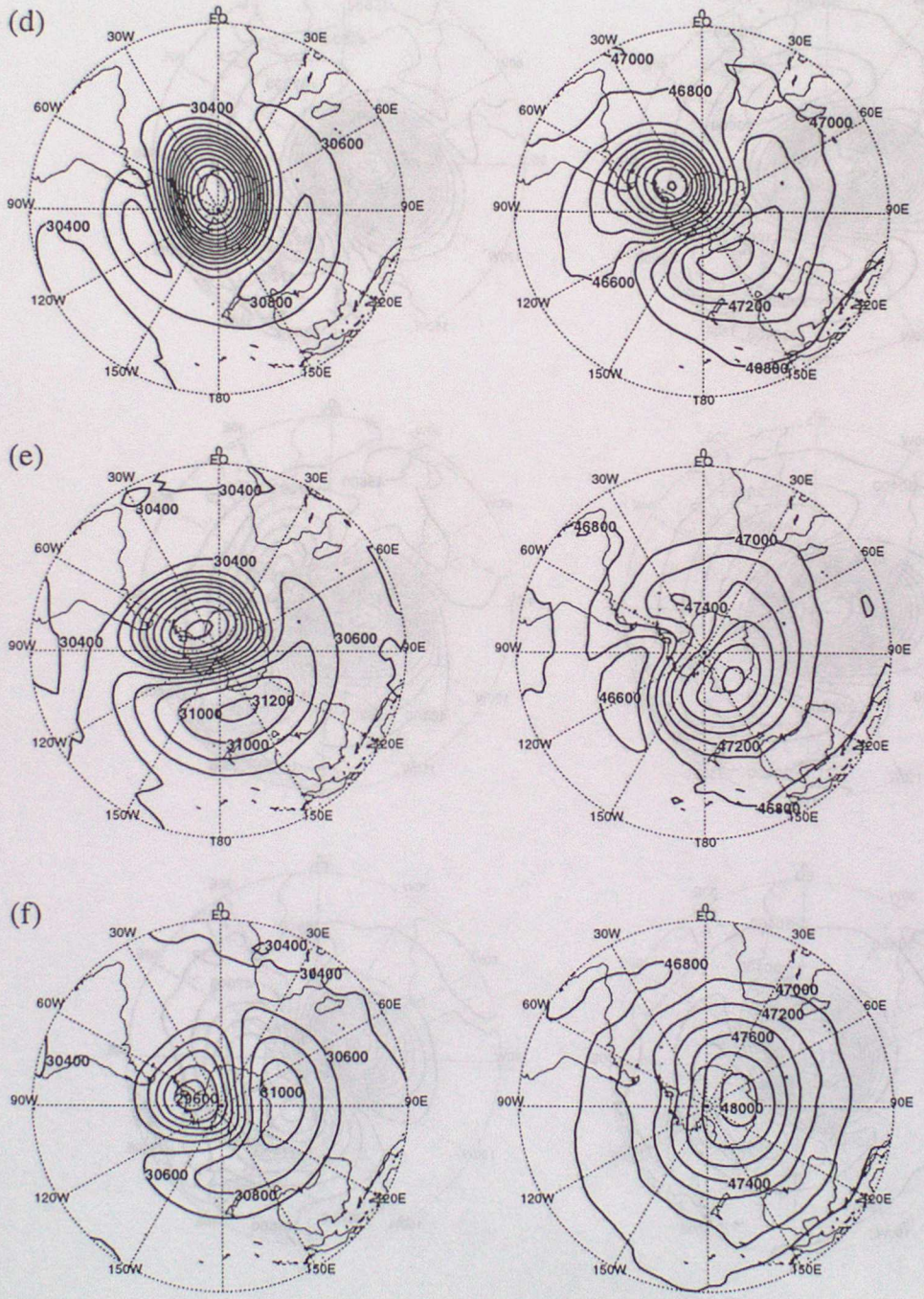

Fig. 19(cont). (d) 22 October 1992; (e) 3 November 1992; (f) 15 November 1992.

Zealand had strengthened considerably. Between mid October and mid November (Figures 19d-f) the polar vortex continued to weaken dramatically at 1hPa and much more slowly at 10 hPa, consistent with a top-down break-up of the polar vortex in the southern winter final warming. As mentioned previously, the southern polar vortex typically breaks-up in a top-down fashion.

4.4 Comparison with EUGCM

Table 4 summarises a comparison of the characteristics of the UM and the EUGCM. The EUGCM data came from two sources: (a) a 10 year T21L47 run; (b) a 1 year T42L47 run. The initial state for both runs is made up from ECMWF analyses for 7 November 1991 below about 10 hPa and temperatures and balanced winds derived from the Improved Stratospheric and Mesospheric Sounder (ISAMS -- see, e.g. Rosier et al. 1994) for the same day between about 10 hPa and 0.01 hPa, with a simple extrapolation above this level. Details about these EUGCM runs can be found in Norton and Thuburn (1996). Further comparisons between the UM and results from other models, including the EUGCM, are planned as part of the international GRIPS (GCM Reality Intercomparison project for SPARC, where SPARC stands for Stratospheric Processes and their Role in Climate) stratospheric modelling project, in which both the UKMO and UGAMP modelling groups are participating.

5. CONCLUSIONS

In this technical report, we have shown that the stratosphere-troposphere configuration of the Unified Model (UM) gives a simulation of the stratospheric circulation that compares well with the UK Meteorological Office (UKMO) stratospheric analyses.

The main features, capabilities and problem areas of the UM are summarised below:

(1) The UM exhibits a very good simulation of the stratospheric circulation and its seasonal evolution. Synoptic features such as warmings and vortex mergers are captured by the model; however, the UM appears to have less high frequency variability than the UKMO analysis.

(2) The model fields are generally cold everywhere, with the bias being particularly strong poleward of the polar night jet; at the model's lower levels, the cold bias is weak. Heating rates calculated with the UM radiation scheme have a cold bias with respect to those calculated using MIDRAD (the radiation scheme used in the Extended UGAMP GCM -- EUGCM).

(3) In northern winter the polar vortex tends to remain close to the pole, even when the stratosphere is disturbed. This feature is present in other UM runs and contributes to the model's polar night jets being too strong.

(4) The winter westerly jets are not sufficiently tilted towards low latitudes in comparison to observations. Simulations with the EUGCM suggest that this behaviour is associated with the use of Rayleigh friction to parametrize gravity wave drag and that it may be alleviated by using more sophisticated parametrizations.

(5) The polar temperature time series show reasonably realistic behaviour in both hemispheres. The strong northern hemisphere warming in January/February is quite realistic.

(6) The evolution during southern winter is synoptically realistic. Although the early development of the polar vortex occurs roughly at the correct time, the break-up of the polar vortex occurs about a month too late. There is evidence of unrealistically high stationary wave amplitudes in July and August -- a behaviour which is more like northern winter. The seasonal evolution of southern winter in the EUGCM happens about a month too late, i.e. the zonal mean winds build up too slowly and decay too slowly.

(7) The UM southern winter polar night jet has a realistic magnitude of about 100 m/s. This is in marked contrast to the GFDL SKYHI model (Hamilton et al. 1995) and the Middle Atmosphere NCAR Community Climate Model (MACCM2 -- Boville 1995) which have southern winter polar night jets with magnitudes of about 120 m/s (at N90 resolution) and about 145 m/s (at T106 resolution), respectively -- these magnitudes are even less realistic at lower reso-

lutions. The reasons for the different behaviour of the models in their simulation of the southern winter are not yet fully understood and will be the subject of future study.

(8) In common with other middle atmosphere GCMs the UM does not simulate the Quasi-Biennial Oscillation (QBO) which is observed in the tropical stratosphere. Instead, it tends to retain the tropical easterly winds in the initial data; any tropical westerly winds in the initial data gradually reduce over a period of several months, leading to an overall easterly bias in the tropical stratosphere.

(8) The UM simulates a Semi-Annual Oscillation (SAO) in the zonal winds near the tropical stratopause. However, the oscillation does not reverse the winds (which are easterly) and, thus, the model winds tend to be too easterly. Other models such as the GFDL SKYHI and NCAR MACCM2 have an SAO with a weak westerly phase.

The UM shows some promising improvements over earlier troposphere-stratosphere-mesosphere models (e.g. the GFDL SKYHI and NCAR MACCM2 models), although it still has some weaknesses (for example, the cold bias which is generally found in the stratosphere) which will be addressed in future work. A notable positive feature of the UM (especially in comparison with other state-of-the-art troposphere-stratosphere-mesosphere models such as the GFDL SKYHI and NCAR MACCM2 models) is the synoptically realistic simulation of the southern winter stratosphere.

ACKNOWLEDGMENTS

Part of the computer time in the experiment described in this technical note was funded through the European Climate Computer Network (ECCN). The development of the stratosphere-troposphere configuration of the UM is supported by the European Commission under contract ENV4-CT095-0123.

REFERENCES

Betts, A. K., and M. J. Miller, 1993: The Betts-Miller scheme. In: The representation of cumulus convection in numerical models of the atmosphere. Eds. K. A. Emanuel and D. J. Raymond, American Meteorological Society.

Boville, B. A., 1995: Middle Atmosphere version of CCM2 (MACCM2) annual cycle and interannual variability. *J. Geophys. Res.*, **100**, 9017-9039.

Coy, L., and R. Swinbank, 1996: The characteristics of stratospheric winds and temperatures produced by data assimilation. Submitted to *J. Geophys. Res.*.

Cullen, M. J. P., and T. Davies, 1991: A conservative split-explicit integration scheme with

fourth-order horizontal advection. *Quart. J. Roy. Met. Soc.*, **117**, 993-1002.
Cullen, M. J. P., 1993: The unified forecast / climate model. *Meteorol. Mag.*, **122**, 81-94.
Fisher, M., 1987: The Met O 20 Stratosphere-Mesosphere Model. Dynamical Climatology Technical Note no. 52, Meteorological Office, London Road, Bracknell RG12 2SZ.
Folland, C. K. and D. E. Parker, 1990: Observed variations of sea surface temperatures. In *Climate-Ocean Interactions* (Oxford), 21-52.
Gray, L. J., M. Blackburn, M. P. Chipperfield, J. D. Haigh, D. Jackson, K. P. Shine, J. Thuburn, and W. Zhong, 1993: First results from a 3-dimensional middle atmosphere model. *Adv. Space Res.*, **13**, 363-372.
Gregory, D., and S. Allen, 1996: A parametrization of convective downdraft: impact on the climate of the Unified Model, in preparation.
Gregory, D., G. J. Shutts, and J. R. Mitchell, 1996: A new gravity wave drag scheme incorporating anisotropic orography and low-level wave breaking: impact upon the climate of the UK Met Office Unified Model, in preparation.
Gregory, D., and P. R. Rowntree, 1990: A mass flux convection scheme with representation of cloud ensemble characteristics and stability-dependent closure. *Mon. Wea. Rev.*, **118**, 1483-1506.
Gregory, D., 1995: Parametrization of momentum transports by convection II: tests in single column and general circulation models. *Quart. J. Roy. Met. Soc.*, submitted.
Hamilton, K., R. J. Wilson, J. D. Mahlman, and L. J. Umscheid, 1995: Climatology of the SKYHI troposphere-stratosphere-mesosphere general circulation model. *J. Atmos. Sci.*, **52**, 5-43.
Heymsfield, A. J., 1977: Precipitation development in stratiform clouds; a microphysical and dynamical study. *J. Atmos. Sci.*, **34**, 367-387.
Joseph, D., 1980: Navy 10' global elevation values. National Center for Atmospheric Research notes on the FNWC terrain data set, NCAR, Boulder, USA.
Juckes, M. N., and A. O'Neill, 1988: Early winter in the northern stratosphere. *Quart. J. Roy. Met. Soc.*, **114**, 1111-1125.
Keating, G. M., D. F. Young, and M. C. Pitts, 1987: Ozone reference models for CIRA. *Adv. Space Res.*, **7**, 105-115.
Kneizys, F. X., E. P. Shettle, L. W. Abreu, J. H. Chetwynd, G. P. Anderson, W. O. Gallery, J. E. A. Selby, and S. A. Clough, 1988: Users guide to LOWTRAN, AFGL.
Lahoz, W. A., A. O'Neill, A. Heaps, V. D. Pope, R. Swinbank, R. S. Harwood, L. Froidevaux, W. G. Read, J. W. Waters, and G. E. Peckham, 1996: Vortex dynamics and the evolution of water vapour in the stratosphere of the southern hemisphere. *Quart. J. Roy. Met. Soc.*, **122**, 423-450.
Lorenc, A. C., R. S. Bell, and B. MacPherson, 1991: The Meteorological Office analysis correction data assimilation scheme. *Quart. J. Roy. Met. Soc.*, **117**, 59-89.
Mac Low, M.-M., and A. P. Ingersoll, 1986: Merging of vortices in the atmosphere of Jupiter: An analysis of voyager images. *Icarus*, **65**, 353-369.
Mechoso, C. R., A. O'Neill, V. D. Pope, and J. D. Farrara, 1988: A study of the stratospheric

final warming of 1982 in the southern hemisphere. *Quart. J. Roy. Met. Soc.*, **114**, 1365-1384.
Milton, S. F., and C. A. Wilson, 1996: The impact of parametrized subgridscale orographic forcing on systematic errors in a global NWP model. *Mon. Wea. Rev.*, submitted.
Morcrette, J.-J., Y. Fouquart, and L. Smith, 1986: Pressure and temperature dependence of the absorption in long wave radiation parametrization. *Contrib. to Atmos. Phys.*, **59**, 455-469.
Morcrette, J.-J., 1990: Impact of changes to the radiation transfer parametrizations plus cloud optical properties in the ECMWF model. *Mon. Wea. Rev.*, **118**, 847-873.
Norton, W. A., and J. Thuburn, 1996: The mesosphere in the extended UGAMP GCM. In: Gravity wave processes and their parametrization in global climate models. Ed. K. Hamilton, Springer-Verlag.
O'Neill, A., V. D. Pope, W. L. Grose, M. Bailey, H. MacLean, and R. Swinbank, 1994: Evolution of the stratosphere during northern winter 1991-92 as diagnosed from UKMO analyses. *J. Atmos. Sci.*, **51**, 2800-2817.
Rosier, S. M., B. N. Lawrence, D. G. Andrews, and F. W. Taylor, 1994: Dynamical evolution of the northern stratosphere in early winter 1991/92, as observed by the Improved Stratospheric and Mesospheric Sounder. *J. Atmos. Sci.*, **51**, 2783-2799.
Shine, K. P., 1987: The middle atmosphere in the absence of dynamical heat fluxes. *Quart. J. Roy. Met. Soc.*, **113**, 603-633.
Shine, K. P., and J. A. Rickaby, 1989: Solar radiative heating due to absorption in ozone. In: Ozone in the atmosphere. Eds. R. D. Bojkov and P. Fabian, Deepak Publishing Co., Hampton, Virginia.
Shutts, G. J., 1990: A new gravity wave drag parametrization scheme for the Unified Model. Technical and Diffusion Note 204, Meteorological Office, London Road, Bracknell RG12 2SZ.
Simmons, A. J., and R. Strüfing, 1983: Numerical forecasts of stratospheric warmings using a model with a hybrid vertical coordinate system. *Quart. J. Roy. Met. Soc.*, **109**, 81-111.
Slingo, A. (Ed.), 1985: Handbook of the Meteorological Office 11-layer atmospheric general circulation model. Vol. 1: Model description. Dynamical Climatology Technical Note no. 29, Meteorological Office, London Road, Bracknell RG12 2SZ.
Slingo, J., 1980: A cloud parametrization scheme derived from GATE data for use with a numerical model. *Quart. J. Roy. Met. Soc.*, **106**, 747-770.
Slingo, A., and R. C. Wilderspin, 1986: Development of a revised longwave radiation scheme for an atmospheric general circulation model. *Quart. J. Roy. Met. Soc.*, **112**, 371-386.
Smith, R. N. B., 1990: A scheme for predicting layer clouds and their water content in a general circulation model. *Quart. J. Roy. Met. Soc.*, **116**, 371-386.
Sundqvist, H., 1978: A parametrization scheme for non-convective condensation including prediction of cloud water content. *Quart. J. Roy. Met. Soc.*, **104**, 677-690.
Swinbank, R., and A. O'Neill, 1994: A stratosphere-troposphere data assimilation system. *Mon. Weather Rev.*, **122**, 686-702.
Unified Model Documentation Paper 1: Cullen, M. J. P., Introduction to the Unified Forecast/Climate Model. Meteorological Office, London Road, Bracknell RG12 2SZ.

Unified Model Documentation Paper 10: Cullen, M. J. P., T. Davies, and M. H. Mawson, 1993: Conservative finite difference schemes for a unified forecast/climate model. Meteorological Office, London Road, Bracknell RG12 2SZ.
Unified Model Documentation Paper 23: Ingram, W. J., S. Woodward, and J. Edwards, 1996: Radiation. Meteorological Office, London Road, Bracknell RG12 2SZ.
Unified Model Documentation Paper 24: Smith, R. N. B., 1993: Subsurface, surface and boundary layer processes. Meteorological Office, London Road, Bracknell RG12 2SZ.
Unified Model Documentation Paper 25: Gregory, D., R. N. B. Smith, P. Cox, 1994: Canopy, surface and soil hydrology. Meteorological Office, London Road, Bracknell RG12 2SZ.
Unified Model Documentation Paper 26: Smith, R. N. B., D. Gregory, J. F. B. Mitchell, and A. C. Bushell, 1995: Large-scale precipitation. Meteorological Office, London Road, Bracknell RG12 2SZ.
Unified Model Documentation Paper 27: Gregory, D., 1990: Convection scheme. Meteorological Office, London Road, Bracknell RG12 2SZ.
Unified Model Documentation Paper 29: Smith, R. N. B., D. Gregory, and C. Wilson, 1994: Calculation of saturated specific humidity and large-scale cloud. Meteorological Office, London Road, Bracknell RG12 2SZ.
Unified Model Documentation Paper 70: Jones, C. P., 1995: Specification of ancillary fields. Meteorological Office, London Road, Bracknell RG12 2SZ.
White, A. A., and R. A. Bromley, 1995: Dynamically consistent, quasi-hydrostatic equations for global models with a complete representation of the Coriolis force. *Quart. J. Roy. Met. Soc.*, **121**, 399-418.
Zabusky, N. J., M. H. Hughes, and K. V. Roberts, 1979: Contour dynamics for the Euler equations in two dimensions. *J. Comput. Phys.*, **30**, 96-106.

TABLES

Table 1: Coefficients defining levels for the 49-level version of the Unified Model.
Table 2: Dynamical processes in 49-level version of the Unified Model.
Table 3: Physical processes in 49-level version of the Unified Model.
Table 4: Summary of the behaviour of the UM and the EUGCM for a number of middle atmosphere features.

Table 1

Coefficients defining levels for the 49-level version of the Unified Model

The pressure of a level is defined by $p_k = a_k \times p_0 + b_k \times p_s$, where p_0 is a reference pressure (1000hPa) and p_s is the surface pressure; $\eta = a_k + b_k$

level no.	layer boundary			level (mid-layer)		
k	η	a	b	η	a	b
1	1.000000	0.000000	1.000000	0.996990	0.000000	0.996990
2	0.994000	0.000000	0.994000	0.974957	0.000000	0.974957
3	0.956000	0.000000	0.956000	0.930417	0.000000	0.930417
4	0.905000	0.000000	0.905000	0.869832	0.000000	0.869832
5	0.835000	0.000000	0.835000	0.792228	0.002644	0.789584
6	0.750000	0.009881	0.740119	0.699575	0.023382	0.676193
7	0.650000	0.040516	0.609484	0.599503	0.060505	0.538998
8	0.550000	0.081227	0.468773	0.504522	0.100090	0.404432
9	0.460000	0.117369	0.342631	0.422103	0.130416	0.291687
10	0.385000	0.141100	0.243900	0.354698	0.147896	0.206802
11	0.325000	0.152555	0.172445	0.299752	0.154740	0.145012
12	0.275000	0.155117	0.119883	0.252261	0.153779	0.098482
13	0.230000	0.150778	0.079222	0.210643	0.146714	0.063929
14	0.191700	0.141344	0.050356	0.175424	0.135574	0.039850
15	0.159500	0.128846	0.030654	0.145851	0.122193	0.023658
16	0.132500	0.114864	0.017636	0.120962	0.107857	0.013104
17	0.109680	0.100385	0.009295	0.099996	0.093469	0.006527
18	0.090530	0.086250	0.004280	0.082540	0.079798	0.002742
19	0.074730	0.073167	0.001563	0.068131	0.067310	0.000821
20	0.061680	0.061358	0.000322	0.056234	0.056155	0.000079
21	0.050910	0.050910	0.000000	0.046414	0.046414	0.000000
22	0.042020	0.042020	0.000000	0.038313	0.038313	0.000000
23	0.034690	0.034690	0.000000	0.031625	0.031625	0.000000
24	0.028630	0.028630	0.000000	0.026101	0.026101	0.000000
25	0.023630	0.023630	0.000000	0.021541	0.021541	0.000000
26	0.019500	0.019500	0.000000	0.017781	0.017781	0.000000
27	0.016100	0.016100	0.000000	0.014679	0.014679	0.000000
28	0.013290	0.013290	0.000000	0.012117	0.012117	0.000000
29	0.010970	0.010970	0.000000	0.010001	0.010001	0.000000
30	0.009053	0.009053	0.000000	0.008254	0.008254	0.000000
31	0.007473	0.007473	0.000000	0.006813	0.006813	0.000000
32	0.006168	0.006168	0.000000	0.005623	0.005623	0.000000
33	0.005091	0.005091	0.000000	0.004641	0.004641	0.000000
34	0.004202	0.004202	0.000000	0.003831	0.003831	0.000000
35	0.003469	0.003469	0.000000	0.003163	0.003163	0.000000
36	0.002863	0.002863	0.000000	0.002610	0.002610	0.000000
37	0.002363	0.002363	0.000000	0.002154	0.002154	0.000000
38	0.001950	0.001950	0.000000	0.001778	0.001778	0.000000
39	0.001610	0.001610	0.000000	0.001468	0.001468	0.000000
40	0.001329	0.001329	0.000000	0.001212	0.001212	0.000000
41	0.001097	0.001097	0.000000	0.001000	0.001000	0.000000
42	0.000905	0.000905	0.000000	0.000816	0.000816	0.000000
43	0.000730	0.000730	0.000000	0.000649	0.000649	0.000000
44	0.000570	0.000570	0.000000	0.000501	0.000501	0.000000
45	0.000435	0.000435	0.000000	0.000380	0.000380	0.000000
46	0.000326	0.000326	0.000000	0.000282	0.000282	0.000000
47	0.000240	0.000240	0.000000	0.000207	0.000207	0.000000
48	0.000175	0.000175	0.000000	0.000147	0.000147	0.000000
49	0.000121	0.000121	0.000000	0.000100	0.000100	0.000000
50	0.000080	0.000080	0.000000			

Table 2

Dynamical Processes

Note: UMDP (in References) denotes Unified Model Documentation Paper

Process	Description	References	Comments
Dynamics	A split-explicit finite difference scheme is used, with three adjustment steps per (15 minute) advection step. In each adjustment step the pressure, temperature and winds are updated using the pressure gradient, the main parts of the Coriolis terms, and the vertical advection of potential temperature. The average horizontal wind over the adjustment steps is used for the subsequent advection step, which uses a Heun advection scheme.	Cullen and Davies (1991) White and Bromley (1995) UMDP 10	The form of the primitive equations used follows White and Bromley
Diffusion	A third order (∇^6) horizontal diffusion is used with an e-folding time of 12 hours for 2 grid-length waves. No vertical diffusion is used in this version of the model.	UMDP 10	

Table 3

Physical Processes

The set of physical parametrizations used in this version of the model are based on those used for the "third climate version" of the Hadley Centre climate model (also designated HADAM2b), but with changes to the long-wave radiation and Rayleigh friction (rather than gravity wave drag) at upper levels.
Note: UMDP (in References) denotes Unified Model Documentation Paper

Process	Description	References	Comments
Short wave Radiation	Downward diffuse beams combined. Includes spectral division and interactive cloud optical properties. Short-wave gaseous absorption is based on LOWTRAN7. Radiatively active gases considered are water vapour, ozone and carbon dioxide. Cloud is low, medium or high. Standard random overlap of clouds is used.	Kneizys et al (1988) Slingo (1980) Slingo (1985) UMDP 23	Increments calculated 8 times per day. Number of spectral bands is 4.
Longwave radiation	Radiatively active gases considered are water vapour, ozone and carbon dioxide. Standard random overlap of clouds is used. Treats effects of major trace gases in a similar way to the ECMWF model.	UMDP 23 Morcrette et al (1986)	Increments calculated 8 times per day. Number of spectral bands is 6.
Gravity Wave Drag	GWD starts at level 3 with a surface parameter (K^{-1}) of 20 km, and continues up to approximately 20 hPa, where a simple Rayleigh friction scheme takes over, with a damping period of one day at the top level (See Fig 2)	Shutts (1990) Milton and Wilson (1996) Gregory, Mitchell and Shutts (1996)	
Large Scale Precipitation	Large scale precipitation forms in association with stratiform cloud. Condensed water vapour is partitioned into cloud liquid water and ice. Liquid precipitation is detmerined from the cloud fraction and the cloud-mean liquid water. Frozen precipitation is determined from the cloud-mean ice content. (Version of code for use with downdraft convection.)	Sunqvist (1978) Heymsfield (1977) UMDP 26	

Convective processes	Penetrative mass flux convection scheme. Applicable to all types of moist convection, and dry convection. Uses a single cloud model, based around parcel theory modified by entrainment and detrainment to represent an ensemble of convective clouds. Described in terms of pressure levels. Includes downdraft as well as updraft, with a parcel excess calculation.	Gregory and Rowntree (1990) Gregory and Allen (1996) Gregory (1995) UMDP 27	
Cloud scheme	The cloud fraction, saturated specific humidity and water content and calculated from cloud-conserved variables and the relationship between cloud fraction and relative humidity.	Smith (1990) UMDP 29	
Boundary layer and surface processes	Rapidly mixed boundary layer with silhouette orographic roughness. Divided into subcomponents: sea ice themodynamics, soil thermodynamics, turbulent surface exchange and boundary layer mixing coefficients, the surface boundary layer and their implicit solution, adjustment of the surface evaporation and sublimation and the surface tempreature increment, and boundary layer cloud.	UMDP 24 Smith (1990)	
Surface Hydrology	Multi layer surface hydrology is used. Includes snow processes, canopy and surface hydrology, and soil hydrology.	UMDP 25	
Orography	Based on U.S. Navy 10 minute (1/6°) resolution dataset	Joseph (1980)	
Sea Surface Temperatures	The standard climatology used is the MOHSST3 historical SST dataset created within the Meteorological Office, based upon data for the years 1951 to 1980	UMDP 70 Folland and Parker (1990)	Updated every 5 days

Sea Ice	Concentration is specified from a monthly climatology from the World data center for Glaciology, based at the University of Colorado. Data for the Arctic covers 1972 to 1984, for the Antarctic, from 1973 to 1984. The data permits any value from 0 to 1, but the Unified Model permits only values of 0 or 1. i.e, no ice, or complete cover of ice. the threshold value is 0.5. For thickness, in the Northern Hemisphere the ice thickness is set to be 2m, and in the Southern Hemisphere 1m.		Updated every 5 days
Ozone	At upper levels (η<0.0225) the CIRA climatology of Keating et al is used. Ozone from re-processed SBUV (dating from 1979-1981) data is used below.	Keating et al (1987) UMDP 23	Updated every 5 days

Table 4
Comparison between UM and EUGCM

The acronyms RF and PSSJ2 below stand for Rayleigh friction and Palmer-Shutts-Swinbank-Jackson (version 2) gravity wave drag schemes.

Feature	UM 2.5° x 3.75°, L49	EUGCM T21/T42L47
Seasonal evolution in the stratosphere	Good. Early development OK in SH, too rapid in NH; break-up OK in NH, too late in SH. The UM has overstrong stationary waves in the SH. Model fields generally cold everywhere.	Good in NH. SH winter happens too late (and later than the UM). Model fields generally cold everywhere. EUGCM too slow at developing the winter jets in both hemispheres.
Stratospheric warmings	Yes. Realistic.	Yes. Unrealistic at T21, more realistic at T42.
Anticyclone mergers in the winter stratosphere	Yes.	Yes.
Winter polar temperature	Too cold (10 hPa).	Too cold (10 hPa).
Strength of polar night jet	Too strong (RF).	Too strong (RF). Improves in NH with PSSJ2.
Stratospheric tropical winds	Too easterly. SAO: westerly phase weak (RF). No QBO.	Realistic SAO (PSSJ2). No QBO.
Tilt in winter polar night jet	No (RF).	No (RF), Yes (PSSJ2).
2-day wave	To be investigated.	No (RF), Yes (PSSJ2).
Tides	To be investigated.	Diurnal tide investigated: it looks reasonably realistic in amplitude and produces a semi-annual variation with maximum amplitude at equinox.
Tropospheric structure	To be investigated.	To be investigated.

CLIMATE RESEARCH TECHNICAL NOTES

CRTN 1	Oct 1990	Estimates of the sensitivity of climate to vegetation changes using the Penman-Monteith equation. P R Rowntree
CRTN 2	Oct 1990	An ocean general circulation model of the Indian Ocean for hindcasting studies. D J Carrington
CRTN 3	Oct 1990	Simulation of the tropical diurnal cycle in a climate model. D P Rowell
CRTN 4	Oct 1990	Low frequency variability of the oceans. C K Folland, A Colman, D E Parker and A Bevan
CRTN 5	Dec 1990	A comparison of 11-level General Circulation Model Simulations with observations in the East Sahel. K Maskell
CRTN 6	Dec 1990	Climate Change Prediction. J F B Mitchell and Qing-cun Zeng
CRTN 7	Jan 1991	Deforestation of Amazonia - modelling the effects of albedo change. M F Mylne and P R Rowntree
CRTN 8	Jan 1991	The role of observations in climate prediction and research. D J Carson
CRTN 9	Mar 1991	The greenhouse effect and its likely consequences for climate change. D J Carson
CRTN 10	Apr 1991	Use of wind stresses from operational N.W.P. models to force an O.G.C.M. of the Indian Ocean. D J Carrington
CRTN 11	Jun 1991	A new daily Central England Temperature series, 1772-1991. D E Parker, T P Legg and C K Folland
CRTN 12	Jul 1991	Causes and predictability of Sahel rainfall variability. D P Rowell, C K Folland, K Maskell, J A Owen, M N Ward

CLIMATE RESEARCH TECHNICAL NOTES

CRTN 13	Jul 1991	Modelling changes in climate due to enhanced CO2, the role of atmospheric dynamics, cloud and moisture. C A Senior, J F B Mitchell, H Le Treut and Z-X Li
CRTN 14	Sep 1991	Sea temperature bucket models used to correct historical SST data in the Meteorological Office. C K Folland
CRTN 15	Aug 1991	Modelling climate change, and some potential effects on agriculture in the U.K. P R Rowntree, B A Callander and J Cochrane
CRTN 16	Aug 1991	The Boreal Forests and Climate G Thomas and P R Rowntree
CRTN 17	Aug 1991	Development of a Stratosphere-Troposphere Data Assimilation System. R Swinbank.
CRTN 18	Sep 1991	A study of asynchronous coupling using a simple climate model. M K Davey.
CRTN 19	Sep 1991	The Oceanic Carbon Cycle. N K Taylor
CRTN 20	Nov 1991	Worldwide ocean-atmosphere surface fields in Sahel wet and dry years using provisionally corrected surface wind data. M N Ward
CRTN 21	Dec 1991	Coupled tropical ocean global atmosphere models at the UKMO. M K Davey, C Gordon, S Ineson and S Lawrence
CRTN 22	Dec 1991	Empirical parameterisation of tropical ocean-atmosphere coupling. M Allen, M K Davey, D L T Anderson and P D Killworth
CRTN 23	Feb 1992	The temporal evolution of Equatorial Currents in the Indian Ocean D L T Anderson, D J Carrington, R A Corry and C Gordon
CRTN 24	Feb 1992	Stratospheric analyses provided by the U.K. Meteorological Office M J Bailey, A O'Neill and V D Pope

CLIMATE RESEARCH TECHNICAL NOTES

CRTN 25	Feb 1992	Modelling interannual variability in the Indian Ocean using momentum fluxes from the UKMO and ECMWF operational weather analyses. D L T Anderson and D J Carrington
CRTN 26	Mar 1992	A GCM simulation of the impact of Amazonian deforestation on climate using an improved canopy representation J Lean and P R Rowntree
CRTN 27	Mar 1992	The parameterization of rainfall interception in GCMs A J Dolman and D Gregory
CRTN 28	Jun 1992	Development of worldwide marine data eigenvectors since 1985 A W Colman
CRTN 29	Jun 1992	A tropical ocean model with reduced physics M K Davey
CRTN 30	Jun 1992	International Temperature Workshop, Boulder, Colorado, USA, 16 January 1992 Edited by D E Parker
CRTN 31	Jul 1992	Simulation of clear-sky outgoing longwave radiation over the oceans using operational analyses A Slingo and M J Webb
CRTN 32	Sep 1992	A prediction of the transient response of climate J M Murphy
CRTN 33	Nov 1992	LEPS scores for assessing climate model simulations and long-range forecasts. C K Folland
CRTN 34	Jan 1993	Stratospheric Data Assimilation System Guide Editer: R Swinbank
CRTN 35	Mar 1993	A Stratosphere-Troposphere Data Assimilation System R Swinbank and A O'Neill
CRTN 36	Mar 1993	Validation of hydrological schemes for climate models against catchment data. P R Rowntree and J Lean

CLIMATE RESEARCH TECHNICAL NOTES

CRTN 37	Apr 1993	Modelling of palaeoclimates: Examples from the recent past J F B Mitchell
CRTN 38	May 1993	A simulation of seasonality in ENSO forecast skill M K Davey, D L T Anderson and S Lawrence
CRTN 39	Jul 1993	ENSO Prediction experiments using a simple ocean-atmosphere model D-H Wu, D L T Anderson and M K Davey
CRTN 40	Sep 1993	Diagnosis of dynamic sea-surface and sea-level changes from the Cox ocean model J M Gregory
CRTN 41	Sep 1993	Seasonal variations of the clear-sky greenhouse effect: the role of changes in atmospheric temperatures and humidities M J Webb, A Slingo and G L Stephens
CRTN 42	Nov 1993	Sea-level changes under increasing atmospheric CO_2 in a transient coupled ocean-atmosphere GCM experiment. J M Gregory
CRTN 43	Dec 1993	Global and regional patterns of climate change: recent predictions for the Arctic P R Rowntree
CRTN 44	Feb 1994	The effect of changing horizontal diffusion in the atmospheric version of the unified climate model C D Hall and R A Stratton
CRTN 45	Mar 1994	Simulation of El-Niño/Southern Oscillation like variability in a global AOGCM and its response to CO_2 increase. S F B Tett
CRTN 46	Apr 1994	Global data required for monitoring climate change. D E Parker and C K Folland
CRTN 47	May 1994	Seasonal uptake of anthropogenic CO_2 in an ocean general circulation model. N K Taylor

CLIMATE RESEARCH TECHNICAL NOTES

CRTN 48	Jun 1994	A tropic-wide oscillation of boreal summer rainfall and patterns of sea-surface temperature. M N Ward, K Maskell, C K Folland, D P Rowell and R Washington
CRTN 49	Jun 1994	Simulation of the tropical Pacific using a simplified ocean model M A Balmaseda, D L T Anderson and M K Davey
CRTN 50	Sep 1994	Simulation of global mean temperature using a box-diffusion climate model P R Rowntree
CRTN 51	Sep 1994	Seasonal dependence of ENSO prediction skill M A Balmaseda, M K Davey and D L T Anderson
CRTN 52	Nov 1994	Simulation of the Indian Monsoon and Tropical Intraseasonal Variability by a General Circulation Model P M Inness and D Gregory
CRTN 53	Mar 1995	A comparison of modelled surface fluxes with climatological estimates. C Gordon and D K Wright
CRTN 54	Mar 1995	The representation of moist convection in atmospheric models. D Gregory
CRTN 55	Mar 1995	A consistent treatment of the evaporation of rain and snow for use in large-scale models D Gregory
CRTN 56	Apr 1995	Workshop on simulations of the Climate of the Twentieth Century using GISST, 28-30 November 1994, Hadley Centre, Bracknell, UK Edited by C K Folland and D P Rowell
CRTN 57	May 1995	Enhanced shortwave cloud radiative forcing due to anthropogenic aerosols. S E Swartz and A Slingo
CRTN 58	May 1995	The simulation of the tropical oceans in models of different horizontal resolution. C Gordon, D K Wright and C M Roberts
CRTN 59	Sep 1995	The water budget of middle latitude continental regions - a modelling and observational study P R Rowntree
CRTN 60	Sep 1995	Intraseasonal variability of the Indian summer monsoon simulated by the Hadley Centre climate model K Ashok, D Gregory and P M Inness

CLIMATE RESEARCH TECHNICAL NOTES

CRTN 61	Sep 1995	Climate simulations with the Unified Model: AMIP runs C D Hall, R A Stratton and M L Gallani
CRTN 62	Nov 1995	Validation of surface parameters over the oceans in climate simulations with the unified model. C D Hall
CRTN 63	Dec 1995	The GISST2.2 sea surface temperature and sea-ice climatology D E Parker, M Jackson and E B Horton
CRTN 64	Dec 1995	Parametrization of momentum transport by convection. II: Tests in single column and general circulation models. D Gregory, R Kershaw and P M Inness
CRTN 65	Jan 1996	Understanding the sensitivity of a GCM simulation of Amazonian deforestation to the specification of vegetation and soil characteristics. J Lean and P R Rowntree
CRTN 66	Jan 1996	On the efficient calculation of infra-red fluxes and cooling rates using the two-stream equations. J M Edwards
CRTN 67	Jan 1996	The second Hadley Centre coupled ocean-atmosphere GCM: Model description, spinup and validation. TC Johns,RE Carnell,JF Crossley,JM Gregory, JFB Mitchell,CA Senior,SFB Tett and RA Wood
CRTN 68	Feb 1996	The sensitivity of climate simulations to the specification of mixed phase clouds D Gregory and D Morris
CRTN 69	Apr 1996	Using an ensemble of Multi-Decadal GCM simulations ro assess potential seasonal predictability D P Rowell
CRTN 70	May 1996	North Atlantic and European Seasonal Predictability using an Ensemble of Multi-Decadal AGCM Simulations J R Davies, D P Rowell and C K Folland
CRTN 71	Jun 1996	A description of the Second Hadley Centre Coupled Model (HADCM2) T C Johns
CRTN 72	Jul 1996	Palaeoclimate Modelling Intercomparison: UKMO GCM simulations for 6kBP and 21kBP C D Hewitt and J F B Mitchell

CLIMATE RESEARCH TECHNICAL NOTES

CRTN 73	Aug 1996	ENSO responses and low frequency weather variability in the North Pacific/American sector 1949-93 A C Renshaw, D P Rowell and C K Folland
CRTN 74	Sep 1996	Version 2.2 of the Global sea-Ice and Sea Surface Temperature data set, 1903-1994 N A Rayner, E B Horton, D E Parker, C K Folland and R B Hackett
CRTN 75	Sep 1996	A new gravity wave drag scheme incorporating anisotropic orography and low level wave breaking : Impact upon the climate of the UK Met Office Unified Model D Gregory, G J Shutts and J R Mitchell
CRTN 76	Nov 1996	Middle atmosphere variability in the UKMO Unified Model R Swinbank, W Lahoz, C Douglas, A Heaps, R Brugge, W Norton, A O'Neill, D Podd